Journal of Statistical Physics, Vol. 49, Nos. 3/4, 1987

Mean Field Kinetic Theory of a Classical Electron Gas in a Periodic Potential. II. Qualitative Analysis of the Mean-Field Solution in One Dimension

Angel Alastuey[1]

Received May 7, 1987; revision received July 8, 1987

A qualitative analysis is made of the static and dynamic behavior of a one-dimensional classical electron gas in a periodic potential in the framework of a mean-field kinetic theory. The mean-field equations have been formally solved elsewhere in terms of the trajectories of one electron in the mean-field equilibrium potential, which determines the local electronic density. Taking advantage of the relative simplicity of the mean-field expressions in one dimension, we study the effects of the temperature upon the local electronic density, the static structure factor, and the spectrum of the fluctuations in the long-wavelength limit. At high temperatures, the system tends to behave like a homogeneous electron gas; however, the collective plasmon mode at zero wavenumber is damped and shifted below the plasma frequency. At low temperatures, the system behaves as an ensemble of independent electrons strongly localized in the neighborhood of the fixed ions that create the periodic potential; the plasmon mode then vanishes. We consider the physical relevance of these predictions. They turn out to be quite reasonable, despite the failure of mean-field theory to predict the phase of the model.

KEY WORDS: Classical electron gas; periodic potential; mean field; equilibrium fluctuations; plasmon mode; damping; shift.

1. INTRODUCTION

In a previous paper[1] (paper I), we established the mean-field equations describing the static and dynamic behavior of a classical electron gas in a periodic potential in d dimensions. This model is made up of point charges

[1] Laboratoire de Physique Théorique et Hautes Energies (Laboratoire associé au Centre National de la Recherche Scientifique), Université de Paris-Sud, 91405 Orsay, France.

0022-4715/87/1100-0685$05.00/0

$-e$ (the electrons) moving in the periodic potential created by smeared charges e (the ions) fixed at the sites of a periodic lattice. It can be viewed as a special version (the fixed-ion model) of the usual Coulomb gas with two mobile species. In paper I, the mean-field equations were formally solved in terms of the trajectories of one electron in the mean-field equilibrium potential associated with the local electronic density. We also studied the long-wavelength behavior of the static and dynamic structure factors computed through the mean-field equations. It results from this study that the system is always a conductor, at all temperatures and for any d, in the framework of the mean-field theory. The present paper (refered as paper II) is devoted to an explicit and systematic analysis of the mean-field solution in one dimension. In particular, the weak and strong coupling regimes are studied in detail.

The equilibrium statistical mechanics of the one-dimensional Coulomb gas can be worked out exactly.[2] This exact solution is used to show that the two-component system is dielectric at all temperatures[2] from a static-screening point of view. For the present fixed-ion model, exact solutions are also available.[3,4] When the ionic charge density is uniform, the model is in a plasma phase at all temperatures.[3] When the former is nonuniform, the model is always dielectric[4] and it should be insulating from a dynamic point of view, if we assume the transport coefficients to be well-defined quantities. Thus, the man-field predictions regarding the phase diagram are completely wrong in one dimension. Nevertheless, as we shall see throughout this paper, the mean-field theory correctly describes some static and dynamic mechanisms. Since these mechanisms are independent of space dimension, the present one-dimensional analysis is particularly useful for understanding the general features of the mean-field solution in higher dimensions.

This paper is organized as follows. In Section 2, we briefly recall what the model is. The local electronic density is computed in terms of elementary functions in Section 3. Its high- and low-temperature forms are investigated. The temperature dependence of the static structure factor is also briefly discussed. In Section 4, we consider the spectrum of the fluctuations in the long-wavelength limit. By taking advantage of the simplicity of the trajectories in one dimension, we first reduce the formal mean-field expressions in favor of more explicit formulas. This reduction allows us to study the behavior of the collective plasmon mode in both high- and low-temperature regimes. We summarize our main results and make some comments in Section 5.

2. THE MODEL

The fixed-ion model in d dimensions has been defined in paper I. Here, the ions are fixed on a line at the positions $X_n = na$, $n \in \mathbb{Z}$, where a is the lattice spacing. The Wigner–Seitz (WS) unit cell is the interval $[-a/2, a/2]$. The mean electron density is $\rho = 1/a$.

In one dimension, the Coulomb interaction potential between two electrons separated by a distance $|x|$ is

$$\phi_c(|x|) = -e^2|x| \tag{2.1}$$

For the sake of simplicity, we consider that the ions are point charges [i.e., $\delta = 0$ in Eq. (I.2.5)]. The corresponding ion–electron interaction potential is

$$\phi_{ie}(|x|) = -\phi_c(|x|) = e^2|x| \tag{2.2}$$

The excess equilibrium properties of the infinite system only depend on the coupling constant $\Gamma = \beta e^2 a$. The natural length and time scales are respectively the lattice spacing a and the inverse of the plasma frequency $\omega_p = (2e^2\rho/m)^{1/2}$. The Debye wavenumber is $\kappa_D = (2\beta e^2\rho)^{1/2}$.

3. THE LOCAL ELECTRONIC DENSITY AND THE STATIC STRUCTURE FACTOR

In this section, we solve the mean-field equilibrium equations (I.3.10), which determine at one and the same time the local electronic density $\rho(x)$ and the potential $V(x)$. Both $\rho(x)$ and $V(x)$ are periodic functions of x/a with period 1, depending on the coupling constant Γ. Their asymptotic forms when $\Gamma \to 0$ or $\Gamma \to \infty$ are investigated. Some considerations about the qualitative behavior of the mean-field structure factor are also given. We conclude the section with a brief discussion about the deficiencies and the successes of the mean-field approach in the description of the static properties of the model.

3.1. Calculation of $\rho(x)$ and $V(x)$

In the present case, the coupled mean-field equations (I.3.10) become

$$\rho(x) = \rho(0) \exp\{-\beta[V(x) - V(0)]\} \tag{3.1}$$

and

$$V(x) = -e^2 \int_{-\infty}^{\infty} dx' \, |x - x'| \left[\rho(x') - \sum_{n=-\infty}^{\infty} \delta(x' - na) \right] \tag{3.2}$$

The solution of (3.1), (3.2) necessarily satisfies the neutrality sum rule

$$\int_{WS} dx\, \rho(x) = \int_{-a/2}^{a/2} dx\, \rho(x) = 1 \tag{3.3}$$

because otherwise $V(x)$ would diverge. This sum rule will be used as a constraint in our method of resolution. Since both $\rho(x)$ and $V(x)$ are periodic and symmetric functions of x, we only have to compute these functions in the interval $[0, a/2]$.

As seen from Eq. (3.2), $V(x)$ is nothing but the electrostatic potential created by the point ions and the electronic charge distribution $-e\rho(x)$. Therefore, $V(x)$ obeys to the one-dimensional Poisson equation

$$\frac{d^2V}{dx^2}(x) = 2e^2\left[\rho(x) - \sum_{n=-\infty}^{\infty} \delta(x-na)\right] \tag{3.4}$$

B taking the restriction of (3.4) to the interval $[0, a/2]$ with $\rho(x)$ replaced by the expression (3.1), we obtain a second-order differential equation for the dimensionless potential $V^*(x) = \beta[V(x) - V(0)]$. This equation is of the Poisson–Boltzmann type and reads

$$\frac{d^2V^*}{dx^2}(x) = -c\kappa_D^2 \exp[-V^*(x)] \tag{3.5}$$

for $0 < x \leqslant a/2$, with the boundary conditions

$$V^*(0^+) = 0 \tag{3.6}$$

$$\frac{dV^*}{dx}(0^+) = \beta e^2 \tag{3.7}$$

which are direct consequences of the definition of V^* and of the Gauss theorem, respectively (the electrostatic field, which is proportional to dV^*/dx, is discontinuous at the points na where the point ions are located). In Eq. (3.5), c is the constant $c = \rho(0)/\rho$. This equation with the boundary conditions (3.6), (3.7) can be solved by standard methods as shown in Appendix A. The electronic density $\rho(x)$ and the mean-field potential $V(x)$ are then computed through

$$\rho(x) = c\rho \exp[-V^*(x)] \tag{3.8}$$

and

$$\begin{aligned} V(x) &= V(0) + k_B T V^*(x) \\ &= -e^2 \int_{-a/2}^{a/2} dx\, |x|\, \rho(x) + k_B T V^*(x) \\ &= -e^2 c\rho \int_{-a/2}^{a/2} dx\, |x| \exp[-V^*(x)] + k_B T V^*(x) \end{aligned} \tag{3.9}$$

[in the expression (3.2) for $V(0)$, the integral over x' can be restricted to WS with the help of the sum rule (3.3)]. The constant c, which plays the role of a free parameter in the present method, is determined by imposing the neutrality constraint

$$\int_{-a/2}^{a/2} dx\, \rho(x) = 2c\rho \int_{0}^{a/2} dx \exp[-V^*(x)] = 1 \tag{3.10}$$

As shown in Appendix A, this constraint leads to the transcendental equation

$$\mathrm{tg}\{\tfrac{1}{4}\Gamma^{1/2}[4c(\Gamma)-\Gamma]^{1/2}\} = \Gamma^{1/2}/[4c(\Gamma)-\Gamma]^{1/2} \tag{3.11}$$

which relates c to the coupling constant Γ. The resulting expressions for $\rho(x)$ and $V(x)$ are

$$\rho(x) = \rho\left[c(\Gamma)-\frac{\Gamma}{4}\right]\left(1+\mathrm{tg}^2\left\{\left(\frac{1}{2}-\frac{|x|}{a}\right)\Gamma^{1/2}\left[c(\Gamma)-\frac{\Gamma}{4}\right]^{1/2}\right\}\right) \tag{3.12}$$

and

$$V(x) = \frac{-e^2 a}{\Gamma}\ln\left(1+\mathrm{tg}^2\left\{\left(\frac{1}{2}-\frac{|x|}{a}\right)\Gamma^{1/2}\left[c(\Gamma)-\frac{\Gamma}{4}\right]^{1/2}\right\}\right) \tag{3.13}$$

for $|x| \leqslant a/2$.

Let us briefly study the variations of $\rho(x)$ and $V(x)$ in the interval $[0, a/2]$. The $\rho(x)$ decreases monotonically from $\rho(0) = \rho c(\Gamma)$ to $\rho(a/2) = \rho[c(\Gamma) - \Gamma/4]$ when x varies from 0 to $a/2$ [$c(\Gamma)$ is always larger than 1 and larger than $\Gamma/4$], whereas $V(x)$ increases monotonically from $V(0) = e^2 a \ln[1 - \Gamma/4c(\Gamma)]/\Gamma$ to $V(a/2) = 0$. Both $\rho(x)$ and $V(x)$ have a kink at the origin $x = 0$ (and at all the points $x = na$), i.e., the first derivatives $d\rho/dx$ and dV/dx are discontinuous at $x = 0$. This is due to the presence of the point ion located at $x = 0$ [by virtue of Gauss's theorem, one has $dV/dx(0^+) = e^2 = -dV/dx(0^-)$]. Furthermore, $d\rho/dx$ and dV/dx vanish at $x = a/2$ (and at all the points $x = na + a/2$). In Figs. 1 and 2 we have drawn the dimensionless quantities $\rho(x)/\rho$ and $V(x)/e^2 a$, respectively, as functions of x/a in the interval $[-1/2, 1/2]$ for several values of Γ [$\rho(x)/\rho$ and $V(x)/e^2 a$ only depend on x/a and Γ, as should be the case].

3.2. Weak and Strong Coupling Regimes

The weak coupling regime corresponds to the limit $\Gamma \to 0$ (high temperatures or high densities). In this limit, $c(\Gamma)$ goes to 1, and the local den-

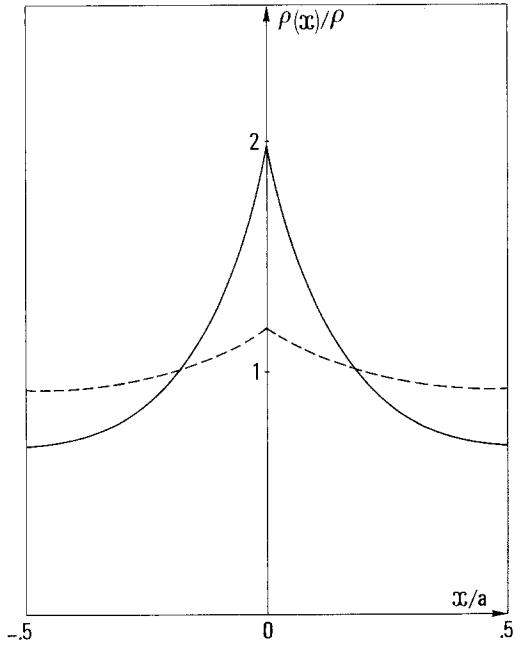

Fig. 1. Plot of $\rho(x)$ as a function of x/a in the interval $[-1/2, 1/2]$. (– –) $\Gamma = 1$; (——) $\Gamma = 5$.

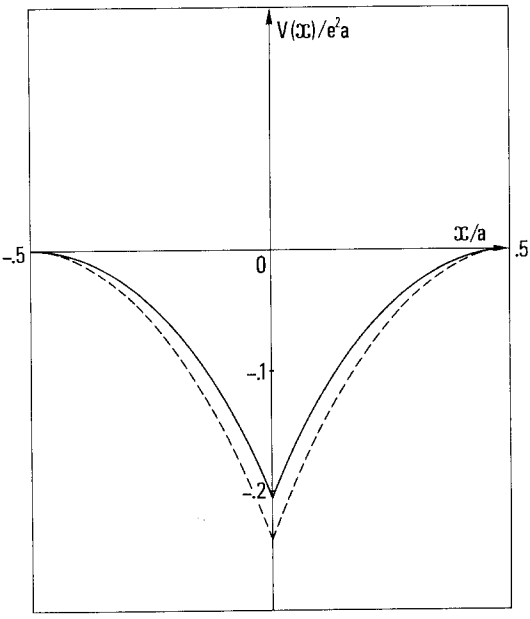

Fig. 2. The same as Fig. 1, with $V(x)/e^2a$ in place of $\rho(x)/\rho$.

sity $\rho(x)$ given by (3.12) becomes uniform and equal to ρ: as expected, the electrons are not sensitive to the periodic structure of the lattice. Replacing $\rho(x')$ by ρ in (3.2), we see that $V(x)$ then reduces to the potential $V_L(x)$ created by the ionic lattice and the uniform charge distribution $-e\rho$, i.e., ($|x| \leqslant a/2$)

$$V(x) \sim V_L(x) = -e^2 a/4 + e^2 |x| - e^2 \rho x^2 \tag{3.14}$$

when $\Gamma \to 0$. Of course, the weak coupling form (3.14) of $V(x)$ can be recovered by taking the limit $\Gamma \to 0$ in (3.13). The corrections to the weak coupling forms of $\rho(x)$ and $V(x)$ are obtained by expanding the expressions (3.12), (3.13) in power series with respect to Γ (x being kept fixed). This gives in particular

$$\rho(x) = \rho \left[1 + \Gamma \left(\frac{1}{6} - \frac{|x|}{a} + \frac{|x^2|}{a^2} \right) + O(\Gamma^2) \right] \tag{3.15}$$

for $|x| \leqslant a/2$.

The strong coupling regime corresponds to the limit $\Gamma \to \infty$ (low temperatures or low densities). In this limit, $c(\Gamma)$ diverges and behaves as $\Gamma/4$. Inserting this asymptotic behavior in (3.12), we find that $\rho(x)$ goes to zero everywhere except at the origin (and at the points $x = na$), where $\rho(0)$ diverges like $\rho\Gamma/4$: the electrons are more and more trapped by the ions as Γ increases, and they are completely frozen at the lattice sites for $\Gamma = \infty$. From (3.13), we infer the large-Γ expansion of the difference $V(x) - V(0)$,

$$V(x) - V(0) \sim e^2 a \left\{ \frac{2}{\Gamma} \ln \Gamma - \frac{1}{\Gamma} \ln \left[4\pi^2 \left(1 + \operatorname{cotg}^2 \frac{x}{a} \right) \right] + o\left(\frac{1}{\Gamma} \right) \right\} \tag{3.16}$$

which is valid for x fixed, $0 < |x| \leqslant a/2$. The strong coupling form of $V(x)$ turns out to be a plateau for $0 < |x| \leqslant a/2$, i.e., $V(x)$ becomes constant in this domain and reduces to $V(0) + 2e^2 a(\ln \Gamma)/\Gamma$ [$V(x)$ varies in a narrow neighborhood of the origin].

3.3. The Static Structure Factor

The mean-field expression (I.5.6) of the static structure factor $S(k)$ here becomes

$$S(k) = k^2 T(k)/[k^2 + \kappa_D^2 T(k)] \tag{3.17}$$

$T(k)$, which is defined by the series (I.5.4), can be rewritten as

$$T(k) = \int_{-a/2}^{a/2} dx\, \rho(x)\, \xi(x; k) \tag{3.18}$$

where $\xi(x;k)$ is the solution of the integral equation

$$\xi(x;k) = 1 - \beta \int_{-a/2}^{a/2} dx'\, \xi(x';k)\, \rho(x')\, \psi_S(x'-x;k) \tag{3.19}$$

with

$$\begin{aligned}
\psi_S(x'-x;k) &= \rho \sum_{\substack{n=-\infty \\ n\neq 0}}^{\infty} \tilde{\phi}_c\left(\left|k - \frac{2\pi n}{a}\right|\right) \exp\frac{2i\pi n(x'-x)}{a} \\
&= 2e^2\rho \sum_{\substack{n=-\infty \\ n\neq 0}}^{\infty} \frac{1}{(k-2\pi n/a)^2} \exp\frac{2i\pi n(x'-x)}{a} \\
&= \frac{e^2 a}{2}\left\{\frac{\exp[ik(x'-x)]}{\sin^2(ak/2)} - 2i\,\mathrm{cotg}\left(\frac{ak}{2}\right)\left(\frac{x'-x}{a}\right)\exp[ik(x'-x)]\right. \\
&\quad \left. - \frac{2|x'-x|}{a}\exp[ik(x'-x)] - \frac{4}{a^2k^2}\right\}, \qquad |x'-x| \leqslant \frac{a}{2}
\end{aligned} \tag{3.20}$$

Note that the static propagator ψ_S is complex. Using the symmetry relations

$$\psi_S(x'-x;k) = \bar{\psi}_S(x-x';k) = \bar{\psi}_S(x'-x;-k), \qquad \rho(-x) = \rho(x)$$

it is easy to check that $T(k)$ and $S(k)$ are real, even functions of k, as they should be [the positivity property of $S(k)$ is hard to prove]. Although the kernel $\rho(x')\,\psi_S(x'-x;k)$ of the integral equation (3.19) is known in terms of elementary functions, we are not able to find a closed analytic expression for $\xi(x;k)$ and consequently for $S(k)$. However, we can study the qualitative dependence of $S(k)$ on both k and Γ.

First, we consider the small-k limit. The function $T(k)$ is an analytic function of k^2 in the vicinity of $k=0$. Furthermore, $T(0)$ is strictly positive at any temperature.[1] Thus, the small-k expansion of $S(k)$ reads

$$S(k) = \frac{k^2}{\kappa_D^2}\left[1 - \frac{k^2}{k_s^2} + O(k^4)\right] \tag{3.21}$$

with $k_s^2 = \kappa_D^2 T(0)$. As usual, k_s^{-1} is identified with the characteristic screening length of the electrons. The ratio $\kappa_D/k_s = 1/[T(0)]^{1/2}$ can be viewed as a measure of the effect of the ionic "trapping" upon the electronic screening. As shown in Appendix B, this ratio is always larger than 1, i.e., the electronic screening is weaker in the present system than in an

homogeneous electron gas. In the weak coupling limit ($\Gamma \to 0$), $T(0)$ goes to 1, while in the strong coupling limit ($\Gamma \to \infty$), $T(0)$ goes to zero: the ionic "trapping" is more and more efficient as Γ increases [Fig. 3 shows the qualitative variations of $T(0)$ as a function of Γ].

When $k \to G_n$ $(n \neq 0)$, the static propagator $\psi_S(x'-x;k)$ becomes singular. However, $T(k)$ remains finite at $k = G_n$, as shown in Appendix B. Moreover, if we introduce the wavenumber $q = k - G_n$ belonging to the first Brillouin zone BZ ($|q| \leqslant \pi/a$), we can express $T(k)$ in terms of the functions $\eta_m(x;q)$ defined as the solutions of the integral equations

$$\eta_m(x;q) = \exp(iG_m x) - \beta \int_{WS} dx'\, \eta_m(x';q)\, \rho(x')\, \psi_S(x'-x;q) \quad (3.22)$$

We find in Appendix B

$$\begin{aligned} T(G_n+q) = ((G_n+q)^2 \{ q^2 T_{n,n}(q) + \kappa_D^2 [T_{0,0}(q)\, T_{n,n}(q) - T_{n,0}(q)\, T_{0,n}(q)] \}) \\ \times \{ (G_n+q)^2 [q^2 + \kappa_D^2 T_{0,0}(q)] - q^2 \kappa_D^2 T_{n,n}(q) \\ - \kappa_D^4 [T_{0,0}(q)\, T_{n,n}(q) - T_{0,n}(q)\, T_{n,0}(q)] \}^{-1} \end{aligned} \quad (3.23)$$

with

$$T_{n,m}(q) = \int_{WS} dx\, \eta_n(x;q)\, \rho(x) \exp(-iG_m x) \quad (3.24)$$

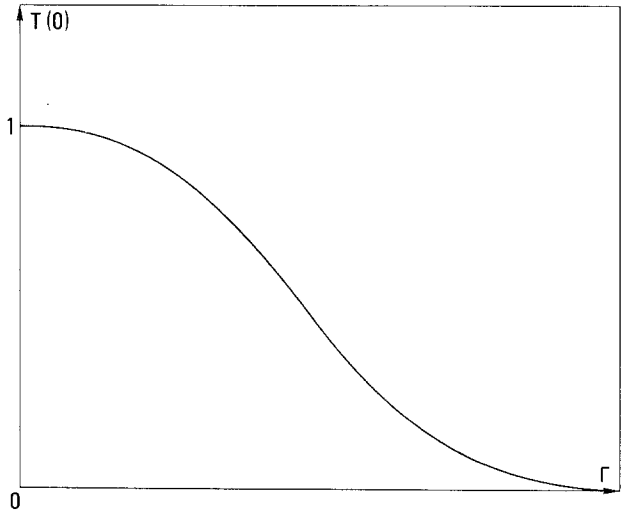

Fig. 3. The qualitative shape of $T(0)$ as a function of Γ.

$[T_{00}(q) = T(q)]$. Since $T_{n,m}(q)$ is a real, analytic function of q in BZ, $T(k) = T(G_n + q)$ and $S(k)$ are analytic functions of k on the real axis. In particular, $T(k)$ is well defined at $k = G_n$ and reduces to

$$T(G_n) = \frac{G_n^2 \kappa_D^2 [T_{0,0}(0)\, T_{n,n}(0) - T_{n,0}(0)\, T_{0,n}(0)]}{G_n^2 \kappa_D^4\, T_{0,0}(0) - \kappa_D^4 [T_{0,0}(0)\, T_{n,n}(0) - T_{n,0}(0)\, T_{0,n}(0)]} \tag{3.25}$$

It can be checked from (3.23) (see Appendix B) that $T(k)$ goes to 1 when $k \to \infty$, and consequently so does $S(k)$, as it should.

The behaviors of $T(G_n)$ in the weak and strong coupling limits give some insight into the Γ dependence of $S(k)$. In Appendix B, the following small-Γ expansions are derived:

$$T(0) = 1 - \frac{\Gamma^3}{3780} + O(\Gamma^4) \tag{3.26}$$

$$T(G_n) = 1 - \frac{4\Gamma^2}{(aG_n)^4} + O(\Gamma^3), \qquad n \neq 0 \tag{3.27}$$

and it is shown that $T(G_n)$ [like $T(0)$] goes to zero when $\Gamma \to \infty$. It results from this that $S(k)$ reduces to the usual Debye–Hückel expression $k^2/(k^2 + \kappa_D^2)$ when $\Gamma \to 0$, while $S(k)$ goes to zero when $\Gamma \to \infty$ (k fixed). Furthermore, $T(k)$ and $S(k)$ should exhibit an oscillating structure for Γ finite (see Appendix B).

In order to give a simple interpretation and a clear meaning to the previous features of $S(k)$, it is useful to investigate their consequences for the two-body distribution function $\rho^{(2)}(x_1, x_2)$ of the electrons. The latter is related to $S(k)$ through

$$S(k) = 1 + \int_{-\infty}^{\infty} dx \exp(ikx) \int_{-a/2}^{a/2} dx_1\, [\rho^{(2)}(x_1, x_1 + x) - \rho(x_1)\, \rho(x_1 + x)] \tag{3.28}$$

Since $S(k)$ is analytic on the real axis, the pair correlation function $h(x)$ averaged over WS,

$$h(x) = a \int_{-a/2}^{a/2} dx_1\, [\rho^{(2)}(x_1, x_1 + x) - \rho(x_1)\, \rho(x_1 + x)] \tag{3.29}$$

decays faster than any inverse power of $|x|$ when $|x| \to \infty$. In fact $h(x)$ should decay exponentially, like $\exp(-|x|/\lambda_s)$, where the screening length λ_s is of the order of k_s^{-1}. When $\Gamma \to 0$, λ_s reduces to the Debye length $\lambda_D = \kappa_D^{-1}$, and when $\Gamma \to \infty$, λ_s becomes of the order of a. The weak coupling form of $h(x)$ merely is $-(\Gamma/2)^{1/2} \exp[-|x|(2\Gamma)^{1/2}/a]$. For Γ

finite, $h(x)$ should oscillate [like $S(k)$]: these oscillations can be traced back to the natural structure imposed by the periodic lattice. The large-Γ behavior of $S(k)$ implies that $h(x)$ vanishes identically when $\Gamma \to \infty$, except in a narow neighborhood of the origin. This means that electrons lying in different cells become uncorrelated in the strong coupling limit. The latter result is compatible with the asymptotic behavior of λ_s.

3.4. Discussion

The mean-field description of the static properties turns out to be quite reasonable from a qualitative point of view. The main reason for this is that the ionic "trapping" is properly taken into account in the mean-field approach. The latter mechanism induces a strong localization of the electrons in the strong coupling limit. In particular, the exact electronic density should become very sharp near the ionic sites when Γ is large. At the same time, the electronic screening should be weakened because the mean density of "free" electrons becomes very small. These expected behaviors of the exact quantities are well reproduced by the mean-field theory. Furthermore, in the weak coupling limit, the mean-field expressions of $\rho(x) - \rho$ and $S(k)$ (for $k \neq 0$) should become asymptotically exact.

Although some aspects of the electronic localization are correctly described by the mean-field theory, it must be borne in mind that the mean-field prediction regarding the phase of the system is wrong for any Γ. This deficiency of the mean-field theory means that the small-k behavior (3.21) does not coincide with the corresponding one of the exact structure factor $S_{\text{exact}}(k)$. In other words, if we define $T_{\text{exact}}(k)$ through (3.17) with $S_{\text{exact}}(k)$ in place of $S(k)$, $T_{\text{exact}}(0)$ is always zero, in contrast to the mean-field $T(0)$, which vanishes only for $\Gamma = \infty$.

Although the system is dielectric[4] for any Γ, the behavior of the exact structure factor has been analyzed introducing notions and quantities, like the electronic screening or the correlation length, that usually characterize a plasma phase. This analysis is allowed because the exact correlations decay like exponentials at large distances.[4] This fact decay is a peculiarity of the one-dimensional system, since in two dimensions, in the dielectric phase, the correlations cannot decay faster[5] than $1/r^4$. This is due to the fact that the electrostatic field created by a compact overall neutral cloud strictly vanishes outside this cloud in one dimension. Finally, let us emphasize that only the charges of the system are screened. On the contrary, infinitesimal external charges are not screened, in agreement with the dielectric nature of the system.

4. THE SPECTRUM OF THE FLUCTUATIONS

In this section, we study the spectrum of the fluctuations in the long-wavelength limit, which is characterized by the function

$$s(\omega) = \lim_{k \to 0} \frac{S(k, \omega)}{S(k)} \tag{4.1}$$

where $S(k, \omega)$ is the dynamic structure factor. The mean-field expression of $s(\omega)$ is[1]

$$s(\omega) = \frac{I(\omega)}{\pi\omega\{[1 + R(\omega)]^2 + I^2(\omega)\}} \tag{4.2}$$

with

$$R(\omega) = \mathrm{Re}\{W_1(\omega) + W_2(\omega)\} \tag{4.3}$$

$$I(\omega) = \mathrm{Im}\{W_1(\omega) + W_2(\omega)\} \tag{4.4}$$

Introducing the complex frequency[2] $\Omega = \omega + i\eta$ $(\eta > 0)$, one has[1] $[\varphi(v) = (\beta m/2\pi)^{1/2} \exp(-\beta m v^2/2)]$

$$W_1(\omega) = -\frac{i\omega}{2} \kappa_D^2 \int_{-a/2}^{a/2} dx \int_{-\infty}^{\infty} dv\, \rho(x)\, \varphi(v) \times \left\{ \lim_{\eta \to 0^+} \int_0^{\infty} dt \exp(i\Omega t)\, [x_{ce}(t; x, v) - x]^2 \right\} \tag{4.5}$$

$$W_2(\omega) = \kappa_D^2 \int_{-a/2}^{a/2} dx'\, \alpha(x'; \omega)\, \rho(x')\, \zeta(x'; \omega) \tag{4.6}$$

where $\alpha(x'; \omega)$ is

$$\alpha(x'; \omega) = i\omega\beta \int_{-a/2}^{a/2} dx \int_{-\infty}^{\infty} dv\, \rho(x)\, \varphi(v) \times \left\{ \lim_{\eta \to 0^+} \int_0^{\infty} dt \exp(i\Omega t)[x_{ce}(t; x, v) - x]\, \psi_S(x' - x_{ce}(t; x, v)) \right\} \tag{4.7}$$

[2] In paper I, the frequency ω is complex and has a finite, positive, imaginary part η, which ensures the convergence of the time integrals $\int_0^{\infty} dt \exp(i\omega t) \cdots$. In the final mean-field expressions, these integrals must be understood as limits when $\eta \to 0^+$. In order to keep the notations as simple as possible, here we redefine the complex frequency as $\Omega = \omega + i\eta$, where henceforth ω is real.

and $\zeta(x';\omega)$ is the solution of the integral equation

$$\zeta(x';\omega)=\gamma(x';\omega)-\beta\int_{-a/2}^{a/2}dx''\,\zeta(x'';\omega)\,\rho(x'')[\psi_S(x''-x')+i\omega\psi_D(x'',x';\omega)] \tag{4.8}$$

with

$$\gamma(x',\omega)=i\omega\int_{-\infty}^{\infty}dv\,\varphi(v)\left\{\lim_{\eta\to 0^+}\int_0^{\infty}dt\exp(i\Omega t)\,[x_{ce}(t;x',v)-x']\right\} \tag{4.9}$$

and

$$\psi_D(x'',x';\omega)=\int_{-\infty}^{\infty}dv\,\varphi(v)\left\{\lim_{\eta\to 0^+}\int_0^{\infty}dt\exp(i\Omega t)\,\psi_S(x''-x_{ce}(t;x',v))\right\} \tag{4.10}$$

$x_{ce}(t;x,v)$ is the position of one electron at time t moving in the mean-field potential $V(x)$ with the initial conditions $x_{ce}(0;x,v)=x$ and $v_{ce}(0;x,v)=v$. It can be easily checked that $s(\omega)$ is a symmetric function of ω (as it should be), i.e., $s(-\omega)=s(\omega)$. Henceforth, we shall study the behavior of $s(\omega)$ for positive frequencies ($\omega>0$).

In Section 4.1 we perform a part of the multiple integrals that determine $W_1(\omega)$ and $W_2(\omega)$ by using simple properties of one-dimensional motions in periodic potentials. The resulting expressions for $W_1(\omega)$ and $W_2(\omega)$ allow us to study the small- and large-ω behavior of $s(\omega)$, as well as its weak and strong coupling forms. The influence of the coupling of the electrons to the ionic lattice upon the collective plasmon mode is also investigated. We conclude the section by a brief discussion about the reliability of the mean-field predictions and their physical meaning.

4.1. Reduction of the Mean-Field Expressions

The trajectories determining the man-field quantities have the following simple properties, which are quite useful in the reduction processes. These trajectories are confined in WS if the energy $E=mv^2/2+V(x)$ is negative [the maximum of $V(x)$ is $V(a/2)=0$], while they are unconfined and go through an infinite number of cells if E is positive. For both confined and unconfined trajectories, the velocity $v_{ce}(t;x,v)$ is a periodic function of the time with a period $T^*_{ce}(E)$ depending only on the energy E,

$$T^*_{ce}(E)=\begin{cases}4T_{ce}(E)=4\displaystyle\int_0^{x_m(E)}dx\left(\frac{m}{2[E-V(x)]}\right)^{1/2}, & E<0\\[2ex] 2T_{ce}(E)=2\displaystyle\int_0^{a/2}dx\left(\frac{m}{2[E-V(x)]}\right)^{1/2}, & 0<E\end{cases} \tag{4.11}$$

In (4.11), $x_m(E)$ is the turning point belonging to $[0, a/2]$ for the confined trajectories ($E<0$), i.e., $x_m(E)$ is such that $V(x_m(E))=E$. The position $x_{ce}(t; x, v)$ obviously obeys the time-translation properties

$$x_{ce}(t+nT^*_{ce}(E); x, v)=\begin{cases} x_{ce}(t; x, v), & E<0 \\ x_{ce}(t; x, v)+n\,\mathrm{sgn}(v)a, & 0<E \end{cases} \tag{4.12}$$

with n integer. The trajectories are entirely determined either by the initial conditions (x, v) or by the variables (E, t_m) and $\mathrm{sgn}(v)$, with

$$t_m=\begin{cases} \displaystyle\int_x^{x_m(E)} dx' \left(\frac{m}{2[E-V(x')]}\right)^{1/2}, & E<0 \\ \displaystyle\int_x^{a/2} dx' \left(\frac{m}{2[E-V(x')]}\right)^{1/2}, & 0<E \end{cases} \tag{4.13}$$

Furthermore, we have the simple relation

$$x_{ce}(t; x, v)=\mathrm{sgn}(v)\, x(t+\mathrm{sgn}(v)\,[T_{ce}(E)-t_m]; E) \tag{4.14}$$

where $x(t; E)$ is the position along the trajectory corresponding to the special initial condition $(0, [2(E-V(0))/m]^{1/2})$, i.e.,

$$x(t; E)=x_{ce}(t; 0, [2(E-V(0))/m]^{1/2})$$

The reduction operations are straightforward and rather tedious. Subsequently, we briefly describe the main steps of these calculations. First, using the periodicity of the velocity and (4.12), the time integrals $\int_0^\infty dt \exp(i\Omega t)\cdots$ are reduced to integrals over the finite interval $[0, T^*_{ce}(E)]$. Note that this reduction involves the calculation of the geometrical series $\sum_{n=0}^\infty \exp[in\Omega T^*_{ce}(E)]$, which is convergent and equal to $1/\{1-\exp[i\Omega T^*_{ce}(E)]\}$ because Ω has a finite, positive, imaginary part. For the mean-field quantities that involve averages over $\mathrm{WS}\otimes\mathbb{R}$ with the weight factor $\rho(x)\,\varphi(v)$, a second reduction is performed. For this purpose, we switch from the variables (x, v) to the variables (E, t_m) ($\mathrm{sgn}\, v$ being given). As shown in Appendix C, the Jacobian $D(x, v)/D(E, t_m)$ merely reduces to $1/m$. In this transformation, the weight factor $\rho(x)\,\varphi(v)$ obviously becomes (part from a constant) $\exp(-\beta E)$, while the integration ranges for E and t_m are $[V(0), \infty]$ and $[0, 2T_{ce}(E)]$, respectively. Using relation (4.14) and the symmetry properties of $x(t; E)$, the multiple integrals

$$\int_{\mathrm{WS}\otimes\mathbb{R}} dx\, dv\, \rho(x)\,\varphi(v) \int_0^\infty dt \exp(i\Omega t)\cdots \tag{4.15}$$

are finally rewritten as simple integrals over E, where the integrants are products of $\exp(-\beta E)$ by time integrals upon $[0, T_{ce}(E)]$ involving $x(t; E)$ and $v(t; E)$. In particular, we find

$$W_1(\omega) = \frac{-4\Gamma^{3/2}\rho(0)\exp[\beta V(0)]\,\omega_p}{\sqrt{\pi}\,e^2 a^2 \omega}$$
$$\times \lim_{\eta \to 0^+} \int_{V(0)}^{\infty} dE \exp(-\beta E)$$
$$\times \left\{ P(\Omega T_{ce}(E)) \left[\int_0^{T_{ce}(E)} dt \cos(\Omega t)\, v(t; E) \right]^2 \right.$$
$$+ \int_0^{T_{ce}(E)} dt \sin(\Omega t)\, v(t; E) \int_0^{T_{ce}(E)} dt \cos(\Omega t)\, v(t; E)$$
$$\left. + \int_0^{T_{ce}(E)} dt' \int_{t'}^{T_{ce}(E)} dt \sin(\Omega t - \Omega t')\, v(t; E)\, v(t'; E) \right\} \quad (4.16)$$

with

$$P(\Omega T_{ce}(E)) = \begin{cases} -tg[\Omega T_{ce}(E)], & E < 0 \\ \operatorname{cotg}[\Omega T_{ce}(E)], & 0 < E \end{cases} \quad (4.17)$$

$W_2(\omega)$ cannot be expressed in a form as compact as (4.16). However, the various ingredients determining $W_2(\omega)$ take the following simplified forms:

$$\alpha(x'; \omega) = -\frac{\Gamma^{3/2}\rho(0)\exp[\beta V(0)]\,\omega_p}{\sqrt{\pi}\,e^4 a}$$
$$\times \lim_{\eta \to 0^+} \int_{V(0)}^{\infty} dE \exp(-\beta E)$$
$$\times \left\{ Q(\Omega; T_{ce}(E)) \int_0^{T_{ce}(E)} dt \sin(\Omega t)\, \psi_S^{(as)}(x', x(t; E)) \right.$$
$$+ \Omega \int_0^{T_{ce}(E)} dt \sin(\Omega t)\, x(t; E) \int_0^{T_{ce}(E)} dt \cos(\Omega t)\, \psi_S^{(as)}(x', x(t; E))$$
$$+ \int_0^{T_{ce}(E)} dt\, x(t; E)\, \psi_S^{(as)}(x', x(t; E))$$
$$\left. + \Omega \int_0^{T_{ce}(E)} dt' \, x(t'; E) \int_0^{t'} dt \sin(\Omega t - \Omega t')\, \psi_S^{(as)}(x', x(t; E)) \right\} \quad (4.18)$$

with

$$\psi_S^{(as)}(x', x) = \psi_S(x' - x) - \psi_S(x' + x) \tag{4.19}$$

and

$$Q(\Omega; T_{ce}(E)) = \begin{cases} \mathrm{tg}[\Omega T_{ce}(E)]\, \Omega \int_0^{T_{ce}(E)} dt \sin(\Omega t)\, x(t; E), & E < 0 \\ -\mathrm{cotg}[\Omega T_{ce}(E)]\, \Omega \int_0^{T_{ce}(E)} dt \sin(\Omega t)\, x(t; E) & \\ \quad - \dfrac{a}{2 \sin[\Omega T_{ce}(E)]}, & 0 < E \end{cases} \tag{4.20}$$

$$\gamma(x'; \omega) = \lim_{\eta \to 0^+} \int_0^\infty dv\, \varphi(v) \frac{1}{\sin[\Omega T_{ce}^*(x', v)/2]} \times \int_0^{T_{ce}^*(x', v)} dt \sin[\Omega t - \Omega T_{ce}^*(x', v)/2]\, v_{ce}(t; x', v) \tag{4.21}$$

and

$$\begin{aligned} &\psi_S(x'' - x') + i\omega \psi_D(x'', x'; \omega) \\ &\quad = -\lim_{\eta \to 0^+} \int_0^\infty dv\, \varphi(v) \frac{1}{\sin[\Omega T_{ce}^*(x', v)/2]} \\ &\qquad \times \int_0^{T_{ce}^*(x', v)} dt \sin\left[\Omega t - \frac{\Omega T_{ce}^*(x', v)}{2}\right] v_{ce}(t; x', v) \\ &\qquad \times \frac{d\psi_S}{ds}\left[x'' - x_{ce}(t; x', v)\right] \end{aligned} \tag{4.22}$$

For η finite, the integrants in $\int_{V(0)}^\infty dE \cdots$ or $\int_0^\infty dv \cdots$ are analytic functions on the real axis. Their analytic continuations in the complex plane have poles located at a distance proportional to η of the real axis. The limits (when $\eta \to 0^+$) of the integrals $\int_{V(0)}^\infty dE \cdots$ and $\int_0^\infty dv \cdots$ can then be obtained by standard methods of the theory of analytical functions. In order to illustrate this, we consider the integral

$$\int_{V(0)}^\infty dE \exp(-\beta E)\, P(\Omega T_{ce}(E)) \left[\int_0^{T_{ce}(E)} dt \cos(\Omega t)\, v(t; E)\right]^2 \tag{4.23}$$

appearing in the expression (4.16) of $W_1(\omega)$. The complex energy is $\mathscr{E} = E + i\mu$ with E and μ real. The singular points of the integrant of (4.23),

which are close to the half straight line ($V(0) \leqslant E$, $\mu = 0$), are simple poles such that

$$\Omega T_{ce}(\mathscr{E}) = \begin{cases} (n+\frac{1}{2})\pi, & V(0) < E < 0 \\ n\pi, & 0 < E \end{cases} \tag{4.24}$$

with n a positive integer. Up to the first order in η, these poles are $\mathscr{E}_{n,<} = E_{n,<} + i\mu_{n,<}$ and $\mathscr{E}_{n,>} = E_{n,>} + i\mu_{n,>}$, where $E_{n,<}$ and $E_{n,>}$ are such that

$$\omega T_{ce}(E_{n,<}) = (n+\tfrac{1}{2})\pi, \qquad V(0) < E_{n,<} < 0 \tag{4.25}$$

and

$$\omega T_{ce}(E_{n,>}) = n\pi, \qquad 0 < E_{n,>} \tag{4.26}$$

respectively, while $\mu_{n,<}$ and $\mu_{n,>}$ are given by

$$\mu_{n,<} = -\frac{(n+1/2)\pi}{\omega^2 \, dT_{ce}/dE(E_{n,<})}\eta \tag{4.27}$$

and

$$\mu_{n,>} = -\frac{n\pi}{\omega^2 \, dT_{ce}/dE(E_{n,>})}\eta \tag{4.28}$$

Since $T_{ce}(E)$ is monotonic increasing for $E<0$ and monotonic decreasing for $E>0$ (see Appendix C), $\mu_{n,<}$ is negative and $\mu_{n,>}$ is positive, i.e., $\mathscr{E}_{n,<}$ is below the real axis and $\mathscr{E}_{n,>}$ is above this axis. Let $\mathscr{C}_\varepsilon$ be the contour oriented as indicated in Fig. 4. The contour $\mathscr{C}_\varepsilon$ is the reunion of the real intervals

$$\begin{aligned} &[V(0), E_{0,<} - \varepsilon\Delta_{0,<}] \\ &[E_{n,<} + \varepsilon\Delta_{n,<}, E_{n+1,<} - \varepsilon\Delta_{n+1,<}], \qquad 0 \leqslant n \\ &[E_{n+1,>} + \varepsilon\Delta_{n+1,>}, E_{n,>} - \varepsilon\Delta_{n,>}], \qquad 0 < n \\ &[E_{1,>} + \varepsilon\Delta_{1,>}, \infty[\end{aligned} \tag{4.29}$$

and of the half-circles

$$\begin{aligned} C_{n,<} &= \{\mathscr{E}; |\mathscr{E} - E_{n,<}| = \varepsilon\Delta_{n,<}, \mu > 0\}, \qquad 0 \leqslant n \\ C_{n,>} &= \{\mathscr{E}; |\mathscr{E} - E_{n,>}| = \varepsilon\Delta_{n,>}, \mu < 0\}, \qquad 0 < n \end{aligned} \tag{4.30}$$

with $\Delta_{n,<} = E_{n+1,<} - E_{n,<}$, $\Delta_{n,>} = E_{n,>} - E_{n+1,>}$, and $0 < \varepsilon < 1$. Because of Cauchy's theorem, one has

$$\int_{V(0)}^{\infty} dE \exp(-\beta E)\, P(\Omega T_{ce}(E)) \cdots = \int_{\mathscr{C}_\varepsilon} d\mathscr{E} \exp(-\beta\mathscr{E})\, P(\Omega T_{ce}(\mathscr{E})) \cdots$$

from which we infer that the limit of (4.23) when $\eta \to 0^+$ reduces to the integral over $\mathscr{C}_\varepsilon$ of the same function with ω in place of Ω. The latter, which does not depend on ε, is computed by taking the small-ε limit; its real and imaginary parts arise from the contributions of the intervals (4.29) and of the half-circles (4.30), respectively. The contributions of (4.29) can be rewritten as a principal part ($\mathscr{P}\mathscr{P}$), while the contributions of (4.30) are given by

$$\frac{-i\pi}{\omega(dT_{ce}/dE)(E_{n,<})} \exp(-\beta E_{n,<}) \left[\int_0^{(n+1/2)\pi/\omega} dt \cos(\omega t)\, v(t; E_{n,<}) \right]^2 \tag{4.31}$$

for $C_{n,<}$ and

$$\frac{i\pi}{\omega(dT_{ce}/dE)(E_{n,>})} \exp(-\beta E_{n,>}) \left[\int_0^{n\pi/\omega} dt \cos(\omega t)\, v(t; E_{n,>}) \right]^2 \tag{4.32}$$

for $C_{n,>}$. The resulting expressions for $\mathrm{Re}\{W_1(\omega)\}$ and $\mathrm{Im}\{W_1(\omega)\}$ are

$$\begin{aligned} \mathrm{Re}\{W_1(\omega)\} = & -\frac{4\Gamma^{3/2}\rho(0)\exp[\beta V(0)]\,\omega_p}{\sqrt{\pi}\, e^2 a^2 \omega} \\ & \times \mathscr{P}\mathscr{P} \int_{V(0)}^{\infty} dE \exp(-\beta E) \left\{ P(\omega T_{ce}(E)) \right. \\ & \times \left[\int_0^{T_{ce}(E)} dt \cos(\omega t)\, v(t; E) \right]^2 \\ & + \int_0^{T_{ce}(E)} dt \sin(\omega t)\, v(t; E) \int_0^{T_{ce}(E)} dt \cos(\omega t)\, v(t; E) \\ & \left. + \int_0^{T_{ce}(E)} dt' \int_{t'}^{T_{ce}(E)} dt \sin(\omega t - \omega t')\, v(t; E)\, v(t'; E) \right\} \end{aligned} \tag{4.33}$$

and

$$\begin{aligned} \mathrm{Im}\{W_1(\omega)\} = & \frac{4\sqrt{\pi}\Gamma^{3/2}\,\rho(0)\exp[\beta V(0)]\,\omega_p}{e^2 a^2 \omega^2} \\ & \times \left\{ \sum_{n=0}^{\infty} \frac{\exp(-\beta E_{n,<})}{(dT_{ce}/dE)(E_{n,<})} \left[\int_0^{(n+1/2)\pi/\omega} dt \cos(\omega t)\, v(t; E_{n,<}) \right]^2 \right. \\ & \left. - \sum_{n=1}^{\infty} \frac{\exp(-\beta E_{n,>})}{(dT_{ce}/dE)(E_{n,>})} \left[\int_0^{n\pi/\omega} dt \cos(\omega t)\, v(t; E_{n,>}) \right]^2 \right\} \end{aligned} \tag{4.34}$$

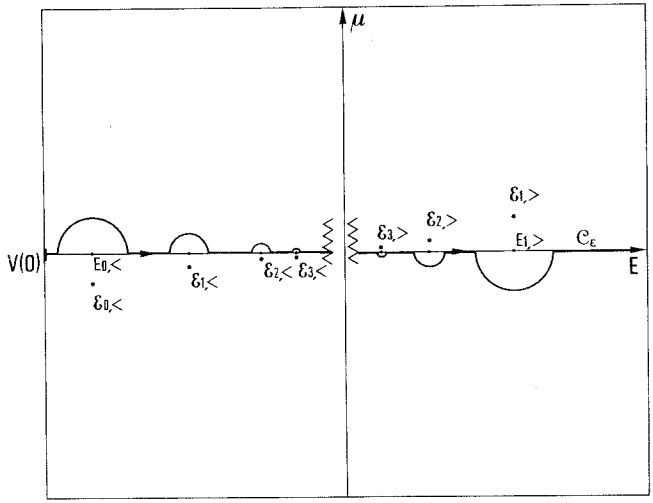

Fig. 4. The oriented countour, $\mathscr{C}_\varepsilon$. The locations in the complex plane (E, μ) of the first poles $\mathscr{E}_{0,<}$, $\mathscr{E}_{1,<}$,... and $\mathscr{E}_{1,>}$, $\mathscr{E}_{2,>}$,... and of the corresponding resonant energies $E_{0,<}$, $E_{1,<}$,... and $E_{1,>}$,... are also indicated.

Similar expressions for the real and imaginary parts of the ingredients (4.18), (4.21), and (4.22) determining $W_2(\omega)$ can be obtained. It is not essential to write down these expressions here.

At a given frequency ω, the imaginary parts of $W_1(\omega)$ and $W_2(\omega)$ arise from the resonant trajectories with the resonant energies $E_{n,>}$ or $E_{n,<}$ satisfying the conditions (4.25), (4.26). These imaginary parts are well-behaved functions of ω, because the singular contributions of $E_{n,<}$ and $E_{n,>}$ are smeared by the Boltzmann-factor-weighted integration over all possible energies. Thus, $s(\omega)$ is a well-behaved, nonvanishing function of ω. This means that the mean-field theory is able to describe dissipation at finite frequencies.

4.2. Low- and Large-Frequency Behavior of $s(\omega)$

First we consider the small-ω limit of $s(\omega)$ (the temperature and the mean density ρ being kept fixed). When $\omega \to 0^+$, the resonant periods $(n+1/2)\pi/\omega$ and $n\pi/\omega$ diverge; the corresponding resonant energies $E_{n,<}$ and $E_{n,>}$ go to zero, while the derivatives $dT_{ce}/dE(E_{n,<})$ and $dT_{ce}/dE(E_{n,>})$ diverge exponentially, as

$$\exp[(2n+1)\pi\,|d^2V/dx^2(a/2)]|^{1/2}/(m^{1/2}\omega)]$$

and

$$\exp[2n\pi\,|d^2V/dx^2(a/2)|^{1/2}/(m^{1/2}\omega)]$$

respectively (see Appendix C). Therefore, the imaginary parts of $W_1(\omega)$, $\alpha(x';\omega)$, $\gamma(x';\omega)$, and $[\psi_S(x''-x')+i\omega\psi_D(x'',x';\omega)]$ decay exponentially. The leading terms of the asymptotic behaviors of the real parts of the previous quantities are obtained by replacing the trigonometric functions involved in (4.33) and (4.20)–(4.22) by their small-ω forms. This shows that $\mathrm{Re}\{W_1(\omega)\}$ is $O(1/\omega^2)$, while $\mathrm{Re}\{\alpha(x';\omega)\}$, $\mathrm{Re}\{\gamma(x';\omega)\}$, and $\mathrm{Re}\{\psi_S(x''-x')+i\omega\psi_D(x'',x';\omega)\}$ are $O(1)$. The previous asymptotic behaviors imply that $\mathrm{Re}\{\zeta(x';\omega)\}$ is $O(1)$ and $\mathrm{Im}\{\zeta(x';\omega)\}$ decays exponentially when $\omega\to 0$. Thus, we finally obtain

$$\mathrm{Re}\{W_1(\omega)\}=O(1/\omega^2) \tag{4.35}$$

$$\mathrm{Re}\{W_1(\omega)\}=O(1) \tag{4.36}$$

whereas $\mathrm{Im}\{W_1(\omega)\}$ and $\mathrm{Im}\{W_2(\omega)\}$ decay exponentially as $\exp(-\mathrm{const}/\omega)$ when $\omega\to 0^+$. Using these behaviors in (4.2)–(4.4), we see that $s(\omega)$ decays exponentially in the zero-frequency limit. Therefore, $s(0)$ does vanish, in agreement with the general (valid in d dimensions) semiheuristic analysis of paper I [note also that the asymptotic behaviors of $W_1(\omega)$ and $W_2(\omega)$ are compatible with the predictions of the latter analysis].

We turn now to the large-ω limit. The large-ω behaviors of the various integrals $\int_0^{T_{ce}(E)} dt\cos(\omega t)\cdots$ and $\int_0^{T_{ce}(E)} dt\sin(\omega t)\cdots$ involved in (4.33) and (4.34) are easily obtained through integrations by parts. These integrals are found to decay like inverse powers of ω. The dominant contributions in (4.33) to $\mathrm{Re}\{W_1(\omega)\}$ arises from $\int_0^{T_{ce}(E)} dt'\int_{t'}^{T_{ce}(E)} dt\cdots$, which is $O(1/\omega)$. Consequently, we have

$$\mathrm{Re}\{W_1(\omega)\}=O(1/\omega^2) \tag{4.37}$$

In (4.34),

$$\int_0^{(n+1/2)\pi/\omega} dt\cos(\omega t)\cdots \qquad \text{and} \qquad \int_0^{n\pi/\omega} dt\cos(\omega t)\cdots$$

turn out to be $O(1/\omega^2)$; furthermore, the discrete sums $\sum_{n=0}^{\infty}\cdots$ and $\sum_{n=1}^{\infty}\cdots$ can be identified with Riemann sums and replaced by the corresponding integrals because the resonant periods $T_{ce}(E_{n,<})$ and $T_{ce}(E_{n,>})$ become closer and closer as ω increases. This gives

$$\mathrm{Im}\{W_1(\omega)\}=O(1/\omega^5) \tag{4.38}$$

The large-ω behavior of the ingredients determining $W_2(\omega)$ can be obtained by similar techniques. When computing the time integrals

involved in (4.18), (4.21), and (4.22) by successive integrations by parts, one has to take into account properly the singular terms arising from the singularities in the second derivatives of $V(s)$ and $\psi_S(s)$ at $s=0$. This makes the large-ω analysis of $W_2(\omega)$ more cumbersome than that of $W_1(\omega)$. We have been content with showing $\mathrm{Re}\{\alpha(x';\omega)\}=O(1)$, $\mathrm{Im}\{\alpha(x',\omega)\}=o(1/\omega^4)$, $\mathrm{Re}\{\gamma(x',\omega)\}=O(1/\omega^2)$, $\mathrm{Im}\{\gamma(x',\omega)\}=o(1/\omega^2)$. Since $\psi_S(x''-x')+i\omega\psi_D(x'',x';\omega)$ is $o(1)$, we see from (4.8) that $\zeta(x';\omega)$ becomes equivalent to $\gamma(x';\omega)$ when $\omega\to\infty$. Taking into account the asymptotic behaviors of $\alpha(x';\omega)$ abd $\gamma(x';\omega)$, we then infer

$$\mathrm{Re}\{W_2(\omega)\}=O(1/\omega^2) \tag{4.39}$$

$$\mathrm{Im}\{W_2(\omega)\}=o(1/\omega^2) \tag{4.40}$$

Inserting (4.37)–(4.40) in (4.2)–(4.4), we finally obtain[3] $s(\omega)=o(1/\omega^3)$ when $\omega\to\infty$.

4.3. The Weak Coupling Limit

Now we study the weak coupling form of $s(\omega)=s(\omega/\omega_p;\Gamma)$ when $\Gamma\to 0$, the ratio ω/ω_p being kept fixed. The previous limit can be reached by different ways in the space of the parameters that define the model and its equilibrium state; all these ways are equivalent insofar as they lead to the same small-Γ expansion of $s(\omega/\omega_p;\Gamma)$. Henceforth, we shall obtain the latter by taking the high-temperature limit ($\beta\to 0$), the other parameters being kept fixed.

Let us consider the case of $W_1(\omega)$. The small-Γ expansion of $\mathrm{Re}\{W_1(\omega)\}$ cannot be immediately obtained from the expression (4.33), for the following reason. If we call $H(E;\omega)$ the term between the braces $\{\cdots\}$ in the integral $\int_{V(0)}^{\infty} dE\exp(-\beta E)\{\cdots\}$ of (4.33), we see that $H(E,\omega)$ diverges as $E^{1/2}$ when $E\to\infty$; therefore, the high-temperature expansion of $\int_{V(0)}^{\infty} dE\exp(-\beta E)H(E;\omega)$ involves divergent terms. In order to handle these terms properly, we first compute the high-energy expansion of $H(E;\omega)$, with the result (see Appendix C)

$$H(E,\omega)=\frac{a}{2\omega}\left(\frac{2E}{m}\right)^{1/2}\left[1-\frac{1}{aE}\int_0^{a/2} dx\,V(x)+O\left(\frac{1}{E^2}\right)\right] \tag{4.41}$$

After splitting the integration range $[V(0),\infty[$ into the intervals $[V(0),0]$ and $[0,\infty]$, we add and subtract to $H(E,\omega)$ the first two terms of (4.41) in $\int_0^{\infty} dE(-\beta E)H(E;\omega)$. The expression (4.33) then becomes

[3] In addition to the algebraic terms arising from $W_1(\omega)$, the asymptotic expansion of $s(\omega)$ when $\omega\to\infty$ might contain nonalgebraic terms arising from $W_2(\omega)$.

$$\mathrm{Re}\{W_1(\omega)\} = -\frac{\omega_p^2}{\omega^2}\frac{\rho(0)}{\rho}\exp[\beta V(0)]\left[1-2\rho\beta\int_0^{a/2} dx\, V(x)\right]$$
$$-\frac{4\Gamma^{3/2}\rho(0)\exp[\beta V(0)]\,\omega_p}{\sqrt{\pi}\,e^2a^2\omega}\mathscr{P}\mathscr{P}\left\{\int_{V(0)}^{0} dE\exp(-\beta E)\,H(E;\omega)\right.$$
$$+\int_0^{\infty} dE\exp(-\beta E)\left[H(E;\omega)-\frac{a}{\omega}\left(\frac{E}{2m}\right)^{1/2}\right.$$
$$\left.\left.+\frac{1}{\omega(2mE)^{1/2}}\int_0^{a/2} dx\, V(x)\right]\right\} \tag{4.42}$$

This expression is particularly suitable for our purpose, because the principal part in the second term of (4.42) remains finite when $\beta \to 0$. The corresponding limit value is merely obtained by replacing $\exp(-\beta E)$ by 1 and $V(x)$ by its weak coupling form, which is nothing but $V_L(x)$ (see Section 3.2). Using also the small-Γ expansions of $\rho(0)$ and of $\exp[\beta V(0)]$, we find

$$\mathrm{Re}(W_1(\omega)) = -\frac{\omega_p^2}{\omega^2} + \Gamma^{3/2} r_{1,0}(\omega) + o(\Gamma^{3/2}) \tag{4.43}$$

when $\Gamma \to 0$; $r_{1,0}(\omega)$ does not depend on Γ and is given by

$$r_{1,0}(\omega) = -\frac{4\omega_p}{\sqrt{\pi}\,e^2a^3\omega}\mathscr{P}\mathscr{P}\left\{\int_{V_L(0)}^{0} dE\, H_L(E;\omega)\right.$$
$$+\int_0^{\infty} dE\left[H_L(E;\omega)-\frac{a}{\omega}\left(\frac{E}{2m}\right)^{1/2}\right.$$
$$\left.\left.+\frac{1}{\omega(2mE)^{1/2}}\int_0^{a/2} dx\, V_L(x)\right]\right\} \tag{4.44}$$

where $H_L(E;\omega)$ is computed with the trajectories in the potential $V_L(x)$. The quadratures over $[0, T_{ce}(E)]$ involved in $H_L(E;\omega)$ can be performed in terms of elementary functions because $v_L(t;E)$ takes a simple form (see Appendix C). The principal part appearing in (4.44) is then transformed into infinite series by using techniques of the theory of analytical functions (see Appendix D). The final expression for $r_{1,0}(\omega)$ is

$$r_{1,0}(\omega) = \frac{\sqrt{\pi}}{2}\frac{\omega\omega_p^3}{(\omega^2+\omega_p^2)^2}\left\{\sum_{n=0}^{\infty}\frac{\mathrm{sh}[(n+1/2)\pi\omega/\omega_p]}{\mathrm{ch}^3[(n+1/2)\pi\omega/\omega_p]}\right.$$
$$\left.+\sum_{n=1}^{\infty}\frac{\mathrm{ch}(n\pi\omega/\omega_p)}{\mathrm{sh}^3(n\pi\omega/\omega_p)}\right\} \tag{4.45}$$

The leading term of the small-Γ expansion of $\mathrm{Im}\{W_1(\omega)\}$ is easily computed from (4.34) by replacing the temperature-dependent quantities by their high-temperature limits. In particular, the potential $V(x)$, which determines the trajectories, is replaced by $V_L(x)$. We find

$$\mathrm{Im}\{W_1(\omega)\} = \Gamma^{3/2} i_{1,0}(\omega) + o(\Gamma^{3/2}) \tag{4.46}$$

when $\Gamma \to 0$, with

$$i_{1,0}(\omega) = \frac{\sqrt{\pi}}{2} \frac{\omega_p^6}{\omega^2(\omega^2+\omega_p^2)^2} \left\{ \sum_{n=0}^{\infty} \frac{\mathrm{sh}[(n+1/2)\pi\omega_p/\omega]}{\mathrm{ch}^3[(n+1/2)\pi\omega_p/\omega]} + \sum_{n=1}^{\infty} \frac{\mathrm{ch}(n\pi\omega_p/\omega)}{\mathrm{sh}^3(n\pi\omega_p/\omega)} \right\} \tag{4.47}$$

and where we have used the simple expressions for $T_{ce}(E)$, $E_{n,<}$, $E_{n,>}$, and $v_L(t; E)$ computed in the ionic potential $V_L(x)$ (see Appendix C).

Now we consider the case of $W_2(\omega)$. The weak coupling form of the ingredients determining $W_2(\omega)$ can be studied by methods similar to those used in the case of $W_1(\omega)$. The term between the braces $\{\cdots\}$ in the expression (4.18) of $\alpha(x'; \omega)$ decays like $1/E^{3/2}$ when $E \to \infty$. This implies that the corresponding integral $\int_{V(0)}^{\infty} dE \exp(-\beta E)\{\cdots\}$ remains finite when $\beta \to 0$. Consequently, $\alpha(x'; \omega)$ is $O(\Gamma^{3/2})$ when $\Gamma \to 0$. Similarly, we obtain from (4.21) $\gamma(x'; \omega) = O(\Gamma^{1/2})$, while $|\psi_S(x''-x') + i\omega\psi_D(x'', x'; \omega)|$ remains bounded when $\Gamma \to 0$. Therefore $\zeta(x'; \omega)$ is $O(\Gamma^{1/2})$. Inserting the weak coupling forms of $\alpha(x'; \omega)$, $\zeta(x'; \omega)$, and $\rho(x')$ in (4.6), we find

$$\mathrm{Re}\{W_2(\omega)\} = O(\Gamma^3) \tag{4.48}$$

$$\mathrm{Im}\{W_2(\omega)\} = O(\Gamma^3) \tag{4.49}$$

when $\Gamma \to 0$.

From the weak coupling behaviors (4.43), (4.46), (4.48), and (4.49) we infer that the contributions of $W_2(\omega)$ to $R(\omega)$ and $I(\omega)$ can be neglected, or in other words that $R(\omega)$ and $I(\omega)$ reduce, respectively, to $\mathrm{Re}\{W_1(\omega)\}$ and $\mathrm{Im}\{W_1(\omega)\}$ up to the order $\Gamma^{3/2}$ included.[4] The resulting weak coupling form of $s(\omega)$ is

$$s(\omega) \sim \Gamma^{3/2}\omega^3 i_{1,0}(\omega) \times (\pi\{(\omega^2-\omega_p^2)^2 + 2\Gamma^{3/2}\omega^2(\omega^2-\omega_p^2) r_{1,0}(\omega) + \Gamma^3\omega^4[r_{1,0}^2(\omega) + i_{1,0}^2(\omega)]\})^{-1} \tag{4.50}$$

[4] This is a particular aspect of a more general result relative to the high-temperature form of the mean-field solution. Indeed, in the high-temperature limit, the density-response function $\chi(k, \omega)$ reduces to[(1)] $\chi_{V_L}^{(0)}(k, \omega)/[1 - \tilde{\phi}_c(k)\chi_{V_L}^{(0)}(k, \omega)]$, where $\chi_{V_L}^{(0)}(k, \omega)$ is the density-response function of independent electrons moving in the potential $V_L(x)$, and $W_1(\omega)$ is nothing but the contribution of $\chi_{V_L}^{(0)}(k, \omega)$ to $s(\omega)$.

when $\Gamma \to 0$, where $r_{1,0}(\omega)$ and $i_{1,0}(\omega)$ are given by (4.45) and (4.47), respectively [both $r_{1,0}(\omega)$ and $i_{1,0}(\omega)$ only depend on the dimensionless parameter ω/ω_p, as they should]. As $\Gamma \to 0$, $s(\omega)$ varies more and more rapidly near the plasma frequency ω_p. For small finite values of Γ, $s(\omega)$ exhibit a peak,[5] centered on the frequency $\omega_m = \omega_p[1 - \Gamma^{3/2} r_{1,0}(\omega_p)/2]$, of height $s(\omega_m) = 1/[\pi\Gamma^{3/2}\omega_p i_{1,0}(\omega_p)]$ and of width proportional to $\Gamma^{3/2}$ (see Fig. 5). Numerically, it is found from the rapidly convergent series (4.45) and (4.47) that $r_{1,0}(\omega_p) = i_{1,0}(\omega_p) \simeq 0.0340$. Replacing ω by $\omega_m + \Gamma^{3/2} v$ in (4.50), we see that $s(\omega)$ has a Lorentzian line shape in the vicinity of ω_m, i.e.,

$$s(\omega_m + \Gamma^{3/2} v) \sim \frac{\omega_p i_{1,0}(\omega_p)}{\pi\Gamma^{3/2}[\omega_p^2 i_{1,0}^2(\omega_p) + 4v^2]} \tag{4.51}$$

when $\Gamma \to 0$. The weak coupling form of $s(\omega)$ is a positive function of ω (as it should be), which does satisfy the elastic and second-moment sum rules,[6] i.e.,

$$\int_{-\infty}^{\infty} d\omega\, s(\omega) = 1 \tag{4.52}$$

and

$$\int_{-\infty}^{\infty} d\omega\, \omega^2 s(\omega) = \omega_p^2 \tag{4.53}$$

when $\Gamma \to 0$.

[5] Of course, for negative frequencies, $s(\omega)$ exhibits a conjugate peak centered on $-\omega_m$.

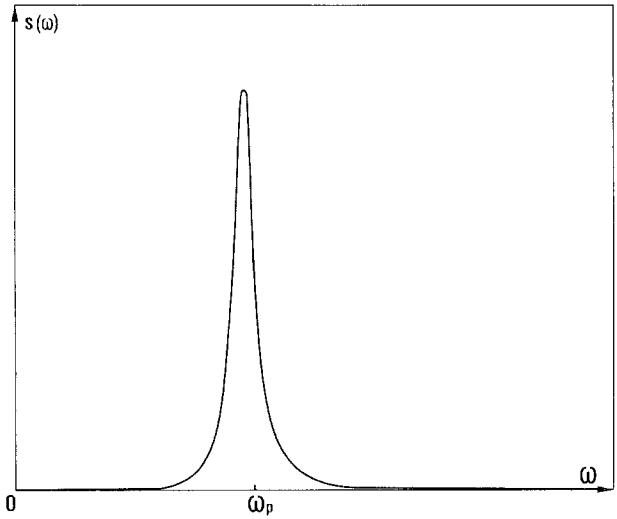

Fig. 5. The qualitative shape of $s(\omega)$ as a function of ω in the weak coupling limit.

The previous analysis shows that, in the weak coupling limit, the spectrum of the fluctuations at $k=0$ is governed mainly by a damped plasmon mode whose frequency is shifted below the plasma frequency ω_p. The shift and the damping are proportional to $\Gamma^{3/2} r_{1,0}(\omega_p)$ and $\Gamma^{3/2} i_{1,0}(\omega_p)$, respectively. They vanish only at $\Gamma=0$; $s(\omega)$ then becomes identical to the usual expression $[\delta(\omega-\omega_p)+\delta(\omega+\omega_p)]/2$ corresponding to a homogeneous electron gas.

4.4. The Strong Coupling Limit

The strong coupling limit of $s(\omega)$ is defined by taking $\Gamma \to \infty$ and by holding ω/ω_p fixed. As in the weak coupling limit (see Section 4.3), the former is equivalent to various other limits, in particular the low-temperature one, $\beta \to \infty$ with the other parameters fixed.

When $\beta \to \infty$, the contributions of the finite-energy trajectories to $W_1(\omega)$ become exponentially small because of the Boltzmann factor $\exp(-\beta E)$. Taking into account the strong coupling form (3.16) of $V(x)$, we have checked that the dominant contributions to $W_1(\omega)$ arise from the confined trajectories with energies

$$E(\lambda) = V(0) + e^2 a \frac{\ln(\Gamma/2\pi)}{\Gamma}\left(1 + 2\frac{\ln(\lambda\omega_p/\omega)}{\ln(\Gamma/2\pi)}\right) \tag{4.54}$$

In the parametric representation (4.54), λ can take all the positive real values. The turning point $x_m(\lambda)$ corresponding to $E(\lambda)$ goes to zero when $\Gamma \to \infty$ (λ fixed) and behaves as $2a\lambda\omega_p/[\omega(2\pi\Gamma)^{1/2}]$, while the period $T_{ce}(\lambda)$ remains finite and reduces to λ/ω. Making the variable change $E \to \lambda$ in (4.33), we then obtain

$$\mathrm{Re}\{W_1(\omega)\} \sim r_{1,\infty}(\omega)/\Gamma^{1/2} \tag{4.55}$$

when $\Gamma \to \infty$. The $r_{1,\infty}(\omega)$ is merely proportional to ω_p/ω with the proportionality constant

$$\begin{aligned} -\frac{8}{\sqrt{\pi}} \mathscr{P}\mathscr{P} \int_0^\infty d\lambda \frac{1}{\lambda} \Bigg\{ -\mathrm{tg}\,\lambda \Bigg[\int_0^1 d\xi \cos\left(\lambda \int_0^\xi d\xi' \frac{1}{[\pi \ln(1/\xi')]^{1/2}}\right)\Bigg]^2 \\ + \int_0^1 d\xi \sin\left(\lambda \int_0^\xi d\xi' \frac{1}{[\pi \ln(1/\xi')]^{1/2}}\right) \\ \times \int_0^1 d\xi \cos\left(\lambda \int_0^\xi d\xi' \frac{1}{[\pi \ln(1/\xi')]^{1/2}}\right) \\ + \int_0^1 d\xi' \int_{\xi'}^1 d\xi \sin\left(\lambda \int_{\xi'}^\xi d\xi'' \frac{1}{[\pi \ln(1/\xi'')]^{1/2}}\right)\Bigg\} \end{aligned} \tag{4.56}$$

which, if necessary, could be evaluated numerically; note that in (4.56) the dimensionless parameter ξ has been introduced by writing $x=\xi x_m(\lambda)$, whereas $\ln(1/\xi')$ comes from the large-Γ expansion of $V(x_m(\lambda))-V(\xi' x_m(\lambda))$. In (4.34), one only has to keep the resonant energies $E_{n,<}$, which obviously correspond to $\lambda_n=(n+1/2)\pi$. We then find

$$\mathrm{Im}\{W_1(\omega)\}\sim i_{1,\infty}(\omega)/\Gamma^{1/2} \tag{4.57}$$

when $\Gamma\to\infty$. Like $r_{1,\infty}(\omega)$, $i_{1,\infty}(\omega)$ is proportional to ω_p/ω with the proportionality constant

$$\frac{8}{\sqrt{\pi}}\sum_{n=0}^{\infty}\frac{1}{n+1/2}\left\{\int_0^1 d\xi\cos\left[\left(n+\frac{1}{2}\right)\pi\int_0^{\xi}d\xi'\frac{1}{[\pi\ln(1/\xi')]^{1/2}}\right]\right\}^2 \tag{4.58}$$

[this constant could be evaluated numerically as for (4.56)].

In (4.6), the dominant contributions to $W_2(\omega)$ arise from the small values of x' proportional to $1/\sqrt{\Gamma}$. The large-Γ behavior of $\alpha(x';\omega)$, $\gamma(x';\omega)$, and $\psi_S(x''-x')+i\omega\psi_D(x'',x';\omega)$ for the arguments $x'=a\xi'/\sqrt{\Gamma}$ and $x''=a\xi''/\sqrt{\Gamma}$ is computed by keeping only the trajectories with energies given by (4.54). This analysis shows that

$$\gamma(a\xi'/\sqrt{\Gamma};\omega)/a$$
$$[\psi_S(a(\xi''-\xi')/\sqrt{\Gamma})+i\omega\psi_D(a\xi''/\sqrt{\Gamma},a\xi'/\sqrt{\Gamma};\omega)]/e^2a$$
$$\alpha(a\xi'/\sqrt{\Gamma};\omega)/a$$

behave as $1/\sqrt{\Gamma}$ times functions of ξ', ξ'', and ω/ω_p. Inserting these behaviors and $a\rho(a\xi''/\sqrt{\Gamma})\sim 1/(\xi'')^2$ in the integral equation (4.8), we see that $\zeta(a\xi'/\sqrt{\Gamma};\omega)/a$ also behaves as $1/\sqrt{\Gamma}$ times a function of ξ' and ω/ω_p. Consequently, we find

$$\mathrm{Re}\{W_2(\omega)\}\sim r_{2,\infty}(\omega)/\Gamma^{1/2} \tag{4.59}$$

$$\mathrm{Im}\{W_2(\omega)\}\sim i_{2,\infty}(\omega)/\Gamma^{1/2} \tag{4.60}$$

when $\Gamma\to\infty$. Both $r_{2,\infty}(\omega)$ and $i_{2,\infty}(\omega)$ depend only on ω/ω_p. They are expressed as integrals similar to (4.6) over ξ' running from $-\infty$ to ∞, the integrants being products of functions of ξ' and ω/ω_p. One of these functions [coming from the large Γ-behavior of $\zeta(a\xi'/\sqrt{\Gamma};\omega)$] is implicitly defined as the solution of an integral equation. If necessary, a numerical analysis of $r_{2,\infty}(\omega)$ and of $i_{2,\infty}(\omega)$ could be easily done.

Inserting (4.55), (4.57), (4.59), and (4.60) in (4.2)–(4.4) we finally obtain

$$s(\omega)\sim\frac{1}{\Gamma^{1/2}}\frac{i_{1,\infty}(\omega)+i_{2,\infty}(\omega)}{\pi\omega} \tag{4.61}$$

when $\Gamma\to\infty$. Thus, at any given frequency ω, $s(\omega)$ goes to zero in the

strong coupling limit. For Γ large and finite, $s(\omega)$ is small everywhere, except in a narrow neighborhood of the origin $\omega = 0$. Indeed, for such values of Γ, the asymptotic expressions (4.55) and (4.57) cannot be used for very small values of ω, because both $r_{1,\infty}(\omega)$ and $i_{1,\infty}(\omega)$ diverge as $1/\omega$ when $\omega \to 0$. This suggests that $s(\omega)$ should exhibit two conjugate peaks near $\omega = 0$ [it must be borne in mind that $s(0) = 0$ for any Γ].

The previous results mean that the collective plasmon mode vanishes when $\Gamma \to \infty$. In this limit, the spectrum of the fluctuations at $k = 0$ is governed by individual damped modes corresponding to the confined oscillations of one electron near its trapping ion.

4.5. Discussion

Unfortunately, a completely unambigous discussion of the mean-field predictions is not possible, because exact (analytic or molecular dynamic) data relative to $s(\omega)$ are not available. However, we claim that these predictions are reliable for the following two reasons. First, they agree, from a qualitative point of view, with molecular dynamic observations in two dimensions.[7] Second, they are consequences of physical mechanisms that are not spurious effects inherent in the mean-field approximation. Subsequently, we summarize the essential mean-field predictions and we discuss their physical meaning.

Since $s(\omega)$ is a well-behaved, nonvanishing function of ω, any density fluctuation at a given frequency $\omega \neq 0$ is damped, even in the infinite-wavelength limit ($k = 0$). This is due to the "friction" of the electrons against the periodic lattice. This damping mechanism has nothing to do with the usual Landau damping for a homogeneous electron gas,[8,9]; in particular, note that the Landau damping vanishes at $k = 0$, in contrast to the present damping, which persists in this limit. In the weak coupling regime, the charge fluctuations at $k = 0$ reduce to collective plasmon oscillations: the ionic "trapping" is weak and the electrons tend to behave as a homogeneous system (with a uniform background) when $\Gamma \to 0$. For Γ small and finite, the plasmon mode is shifted and damped because of the "friction" mechanism. The corresponding shift and damping given by the mean-field theory should become asymptotically exact when $\Gamma \to 0$; in other words, the leading term of a systematic small-Γ expansion of $s_{\text{exact}}(\omega)$ should coincide with the mean-field expression (4.51) in the vicinity of the plasma frequency.[6] The infinite-wavelength plasmons are

[6] In the vicinity of $\omega = 0$, the mean-field description of $s(\omega)$ is of course completely wrong, since $s_{\text{exact}}(0)$ is always infinite. This defect persists at low temperatures, although mean-field theory reproduces some qualitative aspects of the strong electronic localization. From a technical point of view, this is due to the fact that, however small the temperature is, the unconfined trajectories give a finite contribution to $s(\omega)$, which makes $s(\omega)$ vanish when $\omega \to 0$.

increasingly damped and shifted toward zero frequency as the coupling strength increases, due to a gradual "trapping" of the electrons by the ions. In the strong coupling regime, the plasmon mode vanishes. The charge fluctuations then arise from small oscillations of one electron in the binding potential created by its trapping ion. Like the mean-field expression of $s(\omega)$, $s_{\text{exact}}(\omega)$ should vanish everywhere when $\Gamma \to \infty$, except in a narrow neighborhood of $\omega = 0$ [$s_{\text{exact}}(0)$ is infinite for any Γ]. However, the analytic structure of the strong coupling form of $s_{\text{exact}}(\omega)$ is surely different from the prediction of the mean-field theory.

Although the mean-field description of $s(\omega)$ turns out to be quite reasonable, this description might suffer from the following defects. Indeed, except in the weak coupling limit (see Section 4.3), the mean-field expression (4.2) might take negative values and violate the elastic and second-moment sum rules (4.52), (4.53). Note that (4.42) is directly satisfied if $1 + R(\Omega) + iI(\Omega)$ does not vanish in the upper complex half-plane (i.e., for η positive); however, the latter proposition is itself rather hard to prove, and the validity of (4.52) in the framework of the mean-field approach remains an open question.

5. CONCLUSION

The present analysis shows that mean-field theory gives a coherent and reasonable description of the static and dynamic properties at finite wavelengths or finite frequencies. This is due to the fact that mean-field theory takes into account, at least qualitatively, the static "*trapping*" of the electrons by the ions, as well as the dynamic "*friction*" of the electrons against the periodic lattice. The combination of these mechanisms leads to the following mean predictions. In the weak coupling regime, where mean-field theory is expected to be asymptotically exact, the electrons are "weakly" localized. Then, the collective plasmon mode, which essentially governs the spectrum of the fluctuations, is *damped* and *shifted* below the plasma frequency. As the strength of the coupling increases, the electrons are more and more trapped by the ions and the plasmon mode gradually vanishes. In the strong coupling regime, the system behaves as an ensemble of independent oscillators corresponding to the *individual* motions of the electrons near their trapping ion.

The success of the previous mean-field predictions is not inconsistent with the failure of mean-field theory to predict the phase of the system (which is always dielectric[4]). Indeed, the latter is determined by the small-k or the small-ω behaviors of $S(k)$ and $s(\omega)$, respectively. A correct description of such behaviors must include correlations or electron–electron collisions,[1] which are precisely neglected in the mean-field

approach. For k and ω finite, these collisions do not have a crucial effect upon the qualitative behavior of $S(k)$ and of $s(\omega)$.

Since the "trapping" and "friction" mechanisms are present in any dimension, the qualitative mean-field predictions, as well as their reliability, should not depend much on space dimension (except for the predictions regarding the phase of the system,[1] of course). In a forthcoming paper (referred to as paper III), we shall study the accuracy of the mean-field solution through a quantitative comparison with molecular dynamic results in two dimensions.

APPENDIX A

In this Appendix, we solve the mean-field equilibrium equations that determine $\rho(x)$ and $V(x)$. First, let us consider the second-order differential equation (3.5) for $V^*(x) = \beta[V(x) - V(0)]$. Multiplying each side of (3.5) by dV^*/dx and integrating from 0 to x, we obtain

$$\frac{1}{2}\left[\left(\frac{dV^*}{dx}\right)^2 - \beta^2 e^4\right] = c\kappa_D^2\{\exp[-V^*(x)] - 1\} \tag{A1}$$

with the help of the boundary conditions (3.6) and (3.7). Because $dV^*/dx(0^+) = \beta e^2$ is positive, $V^*(x)$ necessarily increases when x increases near $x = 0$. It can be checked by using (A1) that dV^*/dx is in fact positive for $x < x_c$ and vanishes at $x = x_c$, where x_c depends on c. For $x < x_c$, (A1) is integrated as

$$\int_0^{V^*(x)} du \frac{1}{[\exp(-u) - 1 + \Gamma/4c]^{1/2}} = 2(c\Gamma)^{1/2}\frac{x}{a} \tag{A2}$$

and x_c is given by

$$x_c = \frac{a}{2(c\Gamma)^{1/2}} \int_0^{u_c} du \frac{1}{[\exp(-u) - 1 + \Gamma/4c]^{1/2}} \tag{A3}$$

with $u_c = -\ln(1 - \Gamma/4c)$. The quadratures appearing in (A2) and (A3) can be computed in terms of elementary functions by switching from the variable u to the variable $w = [\exp(-u) - 1 + \Gamma/4c]^{1/2}$. This gives

$$V^*(x) = -\ln\left(1 - \frac{\Gamma}{4c}\right) - \ln\left\{1 + \mathrm{tg}^2\left[\mathrm{arctg}\left(\frac{\Gamma}{4c - \Gamma}\right)^{1/2} - \frac{\Gamma^{1/2}}{2}(4c - \Gamma)^{1/2}\frac{x}{a}\right]\right\} \tag{A4}$$

for $x \leqslant x_c$ with

$$x_c = a \frac{2}{\Gamma^{1/2}(4c-\Gamma)^{1/2}} \operatorname{arctg}\left(\frac{\Gamma}{4c-\Gamma}\right)^{1/2} \tag{A5}$$

For $x > x_c$, dV^*/dx becomes strictly neative and $V^*(x)$ is given by an expression different from (A4) (it is not necessary to write this expression here).

Up to now, c is a free parameter. This parameter is determined by imposing the neutrality constraint (3.10). By virtue of Gauss's theorem, this constraint is equivalent to setting $dV^*/dx(a/2) = 0$, or, according to the previous analysis, $x_c = a/2$. This gives the transcendental equation (3.11) for $c(\Gamma)$. Replacing $V^*(x)$ by (A4) in (3.8) and (3.9), we finally obtain the mean-field expressions (3.12) and (3.13) of $\rho(x)$ and $V(x)$, respectively.

APPENDIX B

In this Appendix, we study some properties of $T(k)$. First, we consider the qualitative variations of $T(0)$ as a function of Γ. When $\Gamma \to 0$, $T(0)$ goes to 1. The small-Γ expansion of $T(0)$ can be easily obtained through the perturbative series

$$T(0) = 1 + \sum_{n=1}^{\infty} (-1)^n \beta^n \int_{(\mathrm{WS})^{n+1}} dx\, dx_1 \cdots dx_n\, \rho(x) \times \prod_{j=0}^{n-1} \rho(x_{j+1})\, \psi_S(x_{j+1} - x_j) \tag{B1}$$

($x_0 = x$). The order with respect of Γ of each term of (B1) is determined by replacing $\rho(x_j)$ by its small-Γ expansion (3.15). Taking into account

$$\beta\psi_S(s) = \Gamma(1/6 - |s|/a + s^2/a^2), \qquad |s| \leqslant a/2 \tag{B2}$$

and

$$\int_{\mathrm{WS}} ds\, \psi_S(s) = 0 \tag{B3}$$

we find

$$(-1)^n \beta^n \int_{(\mathrm{WS})^{n+1}} dx \cdots = O(\Gamma^{2n+1})$$

Therefore, the first correction to 1 in (B1) is given by the term $n=1$, which is $O(\Gamma^3)$, i.e.,

$$-\beta \int_{(\mathrm{WS})^2} dx\, dx_1\, \rho(x)\, \rho(x_1)\, \psi_S(x_1 - x)$$

$$\sim -\beta^3 \rho^2 \int_{(\mathrm{WS})^2} dx\, dx_1\, \psi_S(x)\, \psi_S(x_1)\, \psi_S(x_1 - x) \tag{B4}$$

Using the Fourier decomposition of $\psi_S(s)$,

$$\psi_S(s) = \sum_{n=-\infty}^{\infty} \hat{\psi}_{S,n} \exp(iG_n s) \tag{B5}$$

with $\hat{\psi}_{S,0} = 0$ and $\hat{\psi}_{S,n} = e^2 a/(2\pi^2 n^2)$ $(n \neq 0)$, we rewrite (B4) as

$$-\beta \int_{(\mathrm{WS})^2} dx\, dx_1\, \rho(x)\, \rho(x_1)\, \psi_S(x_1 - x)$$

$$\sim -\beta^3 \sum_{n=-\infty}^{\infty} (\hat{\psi}_{S,n})^3 = \frac{-\Gamma^3}{4\pi^6} \sum_{n=1}^{\infty} \frac{1}{n^6} = -\frac{\Gamma^3}{3780} \tag{B6}$$

Using (B6) in (B1), we obtain the small-Γ expansion (3.26) of $T(0)$ up to the order Γ^3 (note that this expansion is an entire series with respect to Γ). In order to study the large-Γ behavior of $T(0)$, it is useful to consider the expression

$$T(0) = \int_{\mathrm{WS}} dx\, \rho(x)\, \xi(x) \tag{B7}$$

where $\xi(x)$ is the solution of the integral equation

$$\xi(x) = 1 - \beta \int_{\mathrm{WS}} dx'\, \xi(x')\, \rho(x')\, \psi_S(x' - x) \tag{B8}$$

When $\Gamma \to \infty$, $\rho(x)$ becomes very sharp near $x=0$ and varies rapidly in a narrow interval of $x=0$ whose amplitude is proportional to $1/\Gamma$; at the same time, for x finite, $\rho(x)$ goes to zero and is $O(1/\Gamma)$. Inserting these behaviors in (B8), it can be checked that $\xi(x)$ is $O(1/\Gamma)$ in the previous interval and remains finite for x finite. We then see from (B7) that $T(0)$ is $O(1/\Gamma)$ when $\Gamma \to \infty$ [the $1/\Gamma$ contributions to $T(0)$ arise from both regions $x = 0(1/\Gamma)$ and x finite]. This strong coupling behavior and the weak coupling expansion (3.26) suggest that $T(0)$ has the qualitative shape drawn in Fig. 3.

Now, we compute $T(G_n+q)$ ($n\neq 0$, $|q|<\pi/a$) in terms of the functions $\eta_m(x;q)$ defined as the solutions of the integral equations (3.22). Replacing $\psi_S(x'-x;\, G_n+q)$ by

$$\psi_S(x'-x;\, G_n+q)=\rho\tilde{\phi}_c(q)\exp[iG_n(x'-x)]-\rho\tilde{\phi}_c(k) + \psi_S(x'-x;\, q)\exp[iG_n(x'-x)] \tag{B9}$$

in (3.19), we obtain ($k=G_n+q$)

$$\xi_n(x;k)=\left[1+\frac{\kappa_D^2}{k^2}\,T(k)\right]\exp(iG_nx)-\frac{\kappa_D^2}{q^2}\,U_n(k) - \beta\int_{WS}dx'\,\xi_n(x';k)\,\rho(x')\,\psi_S(x'-x;q) \tag{B10}$$

with

$$\xi_n(x;k)=\xi(x;k)\exp(iG_nx) \tag{B11}$$

and

$$U_n(k)=\int_{WS}dx\,\xi_n(x;k)\,\rho(x) \tag{B12}$$

Since (B10) is an inhomogeneous linear integral equation for $\xi_n(x;k)$ with the same kernel as (3.22), $\xi_n(x;k)$ reduces to the following linear combination of $\eta_n(x;q)$ and $\eta_0(x;q)$:

$$\xi_n(x;k)=\left[1+\frac{\kappa_D^2}{k^2}\,T(k)\right]\eta_n(x;q)-\frac{\kappa_D^2}{q^2}\,U_n(k)\,\eta_0(x;q) \tag{B13}$$

Furthermore, $U_n(k)$ can be expressed in terms of $T(k)$, $T_{0,0}(q)$, and $T_{n,0}(q)$ by replacing $\xi_n(x;k)$ by (B13) in (B12). This gives

$$U_n(k)=\frac{q^2[k^2+\kappa_D^2\,T(k)]}{k^2[q^2+\kappa_D^2\,T_{0,0}(q)]}\,T_{n,0}(q) \tag{B14}$$

Using (B11) and (B14), we infer from (B13)

$$\xi(x;k)=\left[1+\frac{\kappa_D^2}{k^2}\,T(k)\right]\eta_n(x;q)\exp(-iG_nx) - \frac{\kappa_D^2[k^2+\kappa_D^2\,T(k)]}{k^2[q^2+\kappa_D^2\,T_{0,0}(q)]}\,T_{n,0}(q)\,\eta_0(x;q)\exp(-iG_nx) \tag{B15}$$

The substitution of $\xi(x;k)$ by (B15) in (3.18) gives an algebraic equation for $T(k)$ whose solution in terms of $T_{0,0}(q)$, $T_{n,0}(q)$, $T_{0,n}(q)$, and $T_{n,n}(q)$ is the expression (3.23).

The weak and strong coupling behaviors of $T(G_n)$ $(n \neq 0)$ are determined through methods similar to the ones used previously in the case of $T(0)$. In the weak coupling limit, we start from the perturbative representation of $\eta_n(x) = \eta_n(x; q=0)$, i.e.,

$$\eta_n(x) = \exp(iG_n x) + \sum_{p=1}^{\infty} (-1)^p \beta^p \int_{(\mathrm{WS})^p} dx_1 \cdots dx_p \exp(iG_n x_p) \times \prod_{j=0}^{p-1} \rho(x_{j+1})\, \psi_S(x_{j+1} - x_j) \tag{B16}$$

which gives

$$\eta_n(x) = \exp(iG_n x) - \beta \hat{\psi}_{S,-n} \exp(iG_n x) + \beta^2 \hat{\psi}^2_{S,-n} \exp(iG_n x) - \beta^2 \exp(iG_n x) \sum_{m=-\infty}^{\infty} \hat{\psi}_{S,m} \hat{\psi}_{S,-m-n} \exp(iG_m x) + O(\beta^3) \tag{B17}$$

with the help of (3.15) and of (B5). Inserting (B17) in the definition (3.24) of $T_{n,m}(0)$, we obtain

$$\begin{aligned} T_{0,0}(0) &= T(0) = 1 + O(\Gamma^3) \\ T_{0,n}(0) &= \frac{\Gamma}{2\pi^2 n^2} - \frac{\Gamma^2}{4\pi^4 n^4} + O(\Gamma^3) \\ T_{n,0}(0) &= \frac{\Gamma}{2\pi^2 n^2} - \frac{\Gamma^2}{4\pi^4 n^4} + O(\Gamma^3) \\ T_{n,n}(0) &= 1 - \frac{\Gamma}{2\pi^2 n^2} + \frac{\Gamma^2}{4\pi^4 n^4} + O(\Gamma^3) \end{aligned} \tag{B18}$$

when $\Gamma \to 0$, which leads to the weak coupling expansion (3.27) of $T(G_n)$. In the strong coupling limit, $\eta_n(x)$ has a behavior similar to $\eta_0(x) = \xi(x)$: $\eta_n(x)$ is $O(1/\Gamma)$ in a narrow neighborhood of $x = 0$, and remains finite for x finite. Therefore $T_{n,m}(0)$ is $O(1/\Gamma)$, and then $T(G_n)$ is also $O(1/\Gamma)$ when $\Gamma \to \infty$ [like $T(0)$]. A similar analysis of $T(G_n + q)$ shows that $T(G_n + q) - 1$ is $O(\Gamma^3)$ when $\Gamma \to 0$, while $T(G_n + q)$ is $O(1/\Gamma)$ when $\Gamma \to \infty$. The fact that $T(G_n + q) - 1$ goes to zero faster than $T(G_n)$ when $\Gamma \to 0$ might constitute a precursor sign of the onset of oscillations in $T(k)$ for finite values of Γ.

For studying the large-k behavior of $T(k)$, it is sufficient to consider

the limit of $T(G_n+q)$ when $n\to\infty$ for any given q in BZ. Defining $\eta_n^{(R)}(x;q)$ through

$$\eta_n(x;q)=\exp(iG_nx)+\eta_n^{(R)}(x;q) \tag{B19}$$

we see that $\eta_n^{(R)}(x;q)$ is the solution of the integral equation

$$\eta_n^{(R)}(x;q)=\delta_n(x;q)-\beta\int_{\mathrm{ws}}dx'\,\eta_n^{(R)}(x';q)\,\rho(x')\,\psi_S(x'-x;q) \tag{B20}$$

with

$$\begin{aligned}\delta_n(x;q)&=-\beta\int_{\mathrm{ws}}dx'\exp(iG_nx')\,\rho(x')\,\psi_S(x'-x;q)\\&=-\beta a\sum_{m=-\infty}^{\infty}\hat{\psi}_{S,m}(q)\,\hat{\rho}_{-n-m}\exp(-iG_mx)\end{aligned} \tag{B21}$$

Since both Fourier components of ψ_S and $\rho(x)$ go to zero for large wavevectors, $\delta_n(x;q)$ goes to zero everywhere (uniformly in x) when $n\to\infty$. This implies a similar behavior for $\eta_n^{(R)}(x;q)$ and consequently we have

$$\eta_n(x;q)=\exp(iG_nx)+o(1) \tag{B22}$$

when $n\to\infty$. Using (B22) as well as the decay of the Fourier components of $\rho(x)$ and $\eta_0(x;q)$ for large wavevectors, we find

$$\begin{aligned}&T_{n,0}(q)\to 0\\&T_{0,n}(q)\to 0,\qquad \text{when}\quad n\to\infty\\&T_{n,n}(q)\to 1\end{aligned} \tag{B23}$$

Using (B23) in (3.23), we finally obtain $\lim_{n\to\infty}T(G_n+q)=1$, which shows that $T(k)$ goes to 1 when $k\to\infty$.

APPENDIX C

In this Appendix, we study some properties of the trajectories in the mean-field equilibrium potential $V(x)$. First, we compute the Jacobian $J=D(x,v)/D(E,t_m)$ of the transformation $(x,v)\to(E,t_m)$. It is convenient to rewrite J as

$$\begin{aligned}J&=[D(E,t_m)/D(x,v)]^{-1}\\&=\left|\frac{\partial E}{\partial x}(x,v)\frac{\partial t_m}{\partial v}(x,v)-\frac{\partial E}{\partial v}(x,v)\frac{\partial t_m}{\partial x}(x,v)\right|^{-1}\end{aligned} \tag{C1}$$

One obviously has $\partial E/\partial x(x, v) = dV/dx$ and $\partial E/\partial v(x, v) = mv$. Furthermore, after rewriting t_m as

$$t_m(x, v) = T_{ce}(E(x, v)) + \int_x^0 dx' \left(\frac{m}{2[E - V(x')]}\right)^{1/2} \tag{C2}$$

we find

$$\frac{\partial t_m}{\partial x}(x, v) = \frac{\partial E}{\partial x}(x, v)\left\{\frac{dT_{ce}}{dE} - \frac{m^{1/2}}{2^{3/2}}\int_x^0 dx' \, [E - V(x')]^{-3/2}\right\} - \frac{1}{v} \tag{C3}$$

and

$$\frac{\partial t_m}{\partial v}(x, v) = \frac{\partial E}{\partial v}(x, v)\left\{\frac{dT_{ce}}{dE} - \frac{m^{1/2}}{2^{3/2}}\int_x^0 dx' \, [E - V(x')]^{-3/2}\right\} \tag{C4}$$

Using (C3) and (C4) in (C1), we obtain $J = 1/m$.

Now, we study the variations of $T_{ce}(E)$ when E varies from $V(0)$ to ∞. We immediately see from (4.11) that $T_{ce}(E)$ monotonically decreases from ∞ to 0 when E varies from 0 to ∞. For $E < 0$, we need to compute dT_{ce}/dE. In order to avoid the divergent terms that would appear in a direct differentiation of (4.11) with respect to E, we first proceed to an integration by parts, with the result

$$T_{ce}(E) = \frac{\{2m[E - V(0)]\}^{1/2}}{dV/dx(0^+)} - \int_0^{x_m(E)} dx \frac{d^2V/dx^2\{2m[E - V(x)]\}^{1/2}}{(dV/dx)^2} \tag{C5}$$

Taking the derivative of (C5) with respect to E, we find

$$\frac{dT_{ce}}{dE} = \left(\frac{m}{2}\right)^{1/2}\left(\frac{1}{dV/dx(0^+)[E - V(0)]^{1/2}} - \int_0^{x_m(E)} dx \frac{d^2V/dx^2}{(dV/dx)^2[E - V(x)]^{1/2}}\right) \tag{C6}$$

Since d^2V/dx^2 is negative in the interval $]0, a/2]$ [see Eq. (3.5)] and $dV/dx(0^+)$ is positive, dT_{ce}/dE is positive for $E < 0$. Therefore, $T_{ce}(E)$ monotonically increases from 0 to ∞ when E varies from $V(0)$ to 0.

The leading term of the asymptotic behavior of $T_{ce}(E)$ when $E \to 0$ is computed by replacing $V(x)$ by

$$\frac{1}{2}\frac{d^2V}{dx^2}\left(\frac{a}{2}\right)\left(x - \frac{a}{2}\right)^2 \tag{C7}$$

in (4.11). This gives

$$T_{ce}(E)=\frac{1}{2}\frac{m^{1/2}}{|d^2V/dx^2(a/2)|^{1/2}}\ln\left[\frac{a^2|d^2V/dx^2(a/2)|}{|E|}\right]+\text{const} \qquad \text{(C8)}$$

when $E\to 0$ [$d^2V/dx^2(a/2)$ is negative]. When $\omega\to 0^+$, the resonant periods diverge and the corresponding resonant energies $E_{n,<}$ and $E_{n,>}$ go to 0. According to (C8), $E_{n,<}$ and $E_{n,>}$ behave then as

$$\text{const}\cdot\exp[-(2n+1)\pi\,|d^2V/dx^2(a/2)|^{1/2}/(m^{1/2}\omega)]$$

and

$$\text{const}\cdot\exp[-2n\pi\,|d^2V/dx^2(a/2)|^{1/2}/(m^{1/2}\omega)]$$

respectively. This implies

$$\begin{aligned}\frac{dT_{ce}}{dE}(E_{n,<})&\sim\text{const}\cdot\exp\left[(2n+1)\pi\frac{|d^2V/dx^2(a/2)|^{1/2}}{m^{1/2}\omega}\right]\\ \frac{dT_{ce}}{dE}(E_{n,>})&\sim\text{const}\cdot\exp\left[2n\pi\frac{|d^2V/dx^2(a/2)|^{1/2}}{m^{1/2}\omega}\right]\end{aligned} \qquad \text{(C9)}$$

when $\omega\to 0^+$. The asymptotic behaviors (C9) are also valid in the limit $n\to\infty$, the other parameters being kept fixed. Note that this ensures an exponentially rapid convergence of the series that determine the imaginary parts of the mean-field quantities [see, for instance, the expression (4.34) of $\mathrm{Im}\{W_1(\omega)\}$].

Since $V(x)$ is bounded, in the limit $E\to\infty$ the laws of motion $x(t;E)$ and $v(t;E)$ can be computed by perturbative techniques, where the reference laws $x_0(t;E)=(2E/m)^{1/2}t=v_0t$ and $v_0(t;E)=(2E/m)^{1/2}=v_0$ correspond to free motion. Starting from the conservation of the energy, a straightforward calculation leads to

$$\begin{aligned}v(t;E)=\left(\frac{2E}{m}\right)^{1/2}&\left\{1-\frac{V(v_0t)}{2E}\right.\\&\left.+\frac{1}{4E^2}\left[\frac{dV}{dx}(v_0t)\int_0^{v_0t}dx\,V(x)-\frac{V^2(v_0t)}{2}\right]+O\left(\frac{1}{E^3}\right)\right\}\end{aligned} \qquad \text{(C10)}$$

$$x(t;E)=v_0t-\frac{1}{2E}\int_0^{v_0t}dx\,V(x)+O\left(\frac{1}{E^2}\right) \qquad \text{(C11)}$$

and

$$T_{ce}(E)=\frac{a}{2}\left(\frac{m}{2E}\right)^{1/2}\left[1+\frac{1}{aE}\int_0^{a/2}dx\,V(x)+O\left(\frac{1}{E^2}\right)\right] \qquad \text{(C12)}$$

[the perturbative expansions (C10) and (C11) are valid for $v_0 t$ fixed]. The large-E behaviors of the various time integrals $\int_0^{T_{ce}(E)} dt$ involved in the mean-field expressions directly follow from (C10)–(C12).

Finally, we integrate the equations of motion in the case where $V(x)$ reduces to $V_L(x)$. Here $V_L(x)$ is the reunion of arcs of parabolas with a negative curvature [see (3.14)] and the force $F_L(x) = -dV_L/dx$ takes the linear form $F_L(x) = -e^2(1-2x/a)$ in the interval $[0, a]$. Newton's equation then becomes a second-order linear differential equation with constant coefficients, which is merely integrated in terms of exponential functions. We find

$$v_L(t; E) = \begin{cases} \left(\dfrac{2|E|}{m}\right)^{1/2} \mathrm{sh}[\omega_p T_{ce,L}(E) - \omega_p t], & -\dfrac{e^2 a}{4} < E < 0 \\ \left(\dfrac{2E}{m}\right)^{1/2} \mathrm{ch}[\omega_p T_{ce,L}(E) - \omega_p t], & 0 < E \end{cases} \tag{C13}$$

for $0 < t < 2T_{ce,L}(E)$ with

$$T_{ce,L}(E) = \begin{cases} \dfrac{1}{\omega_p} \mathrm{argch}\left(\dfrac{e^2 a}{4|E|}\right)^{1/2}, & -\dfrac{e^2 a}{4} < E < 0 \\ \dfrac{1}{\omega_p} \mathrm{argsh}\left(\dfrac{e^2 a}{4E}\right)^{1/2}, & 0 < E \end{cases} \tag{C14}$$

[$V_L(0) = -e^2 a/4$]. The resonant energies in $V_L(x)$ are explicitly computed from (C14) as

$$E_{n,<} = -\frac{e^2 a}{4\,\mathrm{ch}^2[(n+1/2)\pi\omega_p/\omega]} \tag{C15}$$

and

$$E_{n,>} = \frac{e^2 a}{4\,\mathrm{sh}^2(n\pi\omega_p/\omega)} \tag{C16}$$

Using (C15) and (C16) in the derivative dT_{ce}/dE calculated from (C14), we obtain

$$\frac{dT_{ce,L}}{dE}(E_{n,<}) = \frac{2}{\omega_p e^2 a} \frac{\mathrm{ch}^3[(n+1/2)\pi\omega_p/\omega]}{\mathrm{sh}[(n+1/2)\pi\omega_p/\omega]} \tag{C17}$$

and

$$\frac{dT_{ce,L}}{dE}(E_{n,>}) = -\frac{2}{\omega_p e^2 a} \frac{\mathrm{sh}^3(n\omega_p/\omega)}{\mathrm{ch}(n\pi\omega_p/\omega)} \tag{C18}$$

The explicit expressions (C13)–(C18) allow one to derive simple representations for $i_{1,0}(\omega)$ [see (4.47)] and $r_{1,0}(\omega)$ (see Appendix D).

APPENDIX D

In this Appendix, we express $r_{1,0}(\omega)$ in terms of infinite series whose convergence is exponentially rapid. We start from the expression (4.44) for $r_{1,0}(\omega)$. In both integrals $\int_{V(0)}^{0} dE\, H_L(E;\omega)$ and $\int_0^\infty dE\, [H_L(E;\omega)+\cdots]$, we switch from the variable E to the dimensionless variable $u=\omega_p T_{ce,L}(E)$. Using (C14), we find the Jacobian $|dE/du|$ of this transformation,

$$\left|\frac{dE}{du}\right| = \begin{cases} \dfrac{e^2 a}{2}\dfrac{\operatorname{sh} u}{\operatorname{ch}^3 u}, & E<0 \\ \dfrac{e^2 a}{2}\dfrac{\operatorname{ch} u}{\operatorname{sh}^3 u}, & 0<E \end{cases} \tag{D1}$$

while the explicit expression (C13) for $v_L(t;E)$ allows us to compute the time integrals $\int_0^{T_{ce,L}(E)} dt\cdots$ in terms of hyperbolic functions. The resulting expression for $r_{1,0}(\omega)$ is

$$\begin{aligned} r_{1,0}(\omega) = {} & \frac{1}{12\sqrt{\pi}}\frac{\omega_p^4(\omega_p^2-\omega^2)}{\omega^2(\omega_p^2+\omega^2)^2} \\ & + \frac{1}{2\sqrt{\pi}}\frac{\omega_p^5}{\omega(\omega_p^2+\omega^2)^2}\,\mathscr{P}\mathscr{P}\int_0^\infty du\,\frac{\operatorname{sh} u}{\operatorname{ch}^3 u}\operatorname{tg}\frac{u\omega}{\omega_p} \\ & - \frac{1}{2\sqrt{\pi}}\frac{\omega_p^5}{\omega(\omega_p^2+\omega^2)^2}\,\mathscr{P}\mathscr{P}\int_0^\infty du\,\frac{\operatorname{ch} u}{\operatorname{sh}^3 u}\left(\operatorname{cotg}\frac{u\omega}{\omega_p}\right. \\ & \left. - \frac{\omega_p}{\omega}\coth u + \frac{\omega_p^2+\omega^2}{3\omega_p\omega}u\right) \end{aligned} \tag{D2}$$

The first principal part appearing in (D2) is transformed as follows. Let $\mathscr{D}_{1,\varepsilon}$ be the contour shown in Fig. 6. We have

$$\begin{aligned} & \mathscr{P}\mathscr{P}\int_0^\infty du\,\frac{\operatorname{sh} u}{\operatorname{ch}^3 u}\operatorname{tg}\frac{u\omega}{\omega_p} \\ & = \frac{1}{2}\operatorname{Re}\left(\lim_{\varepsilon\to 0^+}\int_{\mathscr{D}_{1,\varepsilon}} dz\,\frac{\operatorname{sh} z}{\operatorname{ch}^3 z}\operatorname{tg}\frac{z\omega}{\omega_p}\right) \\ & = \frac{\omega}{4\omega_p}\operatorname{Re}\left(\lim_{\varepsilon\to 0^+}\int_{\mathscr{D}_{1,\varepsilon}} dz\,\frac{1}{\operatorname{ch}^2 z\cos^2(z\omega/\omega_p)}\right) \end{aligned} \tag{D3}$$

where the last line results from an integration by parts. The function $1/[\operatorname{ch}^2 z\cos^2(z\omega/\omega_p)]$ is analytic in the upper ($\operatorname{Im} z>0$) complex half-plane, except at the points $i\pi(n+1/2)$ (n a positive integer) located on the imaginary axis, which are double poles. Furthermore, since this function

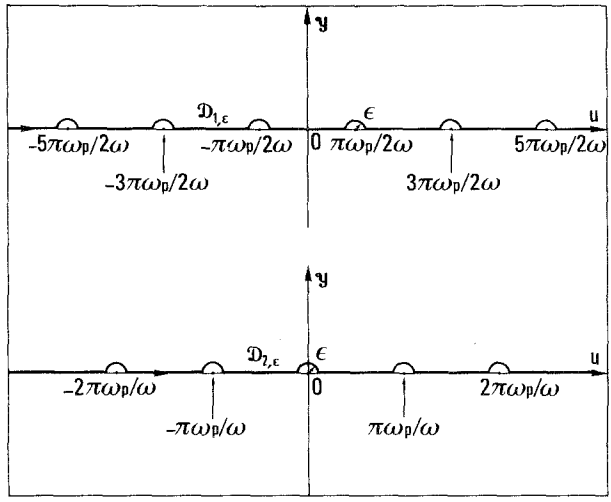

Fig. 6. The oriented contours $\mathfrak{D}_{1,\varepsilon}$ and $\mathfrak{D}_{2,\varepsilon}$ in the complex plane (u, y).

satisfies the hypothesis of Jordan's lemma on the big half-circle $C_N = \{z; |z| = N\pi \text{ and } \operatorname{Im} z \geqslant 0\}$, the integral $\int_{\mathfrak{D}_{1,\varepsilon}} dz \cdots$ appearing in (D3) can be computed by the theorem of residues. This gives

$$\mathscr{P}\mathscr{P}\int_0^\infty du \frac{\operatorname{sh} u}{\operatorname{ch}^3 u} \operatorname{tg}\frac{u\omega}{\omega_p} = \frac{\pi\omega^2}{\omega_p^2} \sum_{n=0}^{\infty} \frac{\operatorname{sh}[(n+1/2)\pi\omega/\omega_p]}{\operatorname{ch}^3[(n+1/2)\pi\omega/\omega_p]} \tag{D4}$$

In order to obtain an expression for the second principal part of (D2) similar to (D4), we first rewrite the latter as

$$\begin{aligned}\mathscr{P}\mathscr{P}\int_0^\infty du \frac{\operatorname{ch} u}{\operatorname{sh}^3 u}\left(\operatorname{cotg}\frac{u\omega}{\omega_p} - \frac{\omega_p}{\omega}\coth u + \frac{\omega_p^2+\omega^2}{3\omega_p\omega}u\right) \\ = \frac{\omega_p^2-\omega^2}{6\omega_p\omega} + \lim_{\varepsilon\to 0^+}\left[\mathscr{P}\mathscr{P}\int_\varepsilon^\infty du \frac{\operatorname{ch} u}{\operatorname{sh}^3 u}\operatorname{cotg}\left(\frac{u\omega}{\omega_p}\right) - \frac{\omega_p}{3\omega\varepsilon^3} + \frac{\omega}{3\omega_p\varepsilon}\right]\end{aligned} \tag{D5}$$

where we have used

$$\begin{aligned}\int_\varepsilon^\infty du \frac{\operatorname{ch}^2 u}{\operatorname{sh}^4 u} &= \frac{\operatorname{ch}\varepsilon}{3\operatorname{sh}^3\varepsilon} + \frac{1}{3}\coth\varepsilon - \frac{1}{3} = \frac{1}{3\varepsilon^3} + \frac{1}{3\varepsilon} - \frac{1}{3} + O(\varepsilon) \\ \int_\varepsilon^\infty du \frac{\operatorname{ch} u}{\operatorname{sh}^3 u} u &= \frac{\varepsilon}{2\operatorname{sh}^2\varepsilon} + \frac{1}{2}\coth\varepsilon - \frac{1}{2} = \frac{1}{\varepsilon} - \frac{1}{2} + O(\varepsilon)\end{aligned} \tag{D6}$$

Let C_ε be the little half-circle $C_\varepsilon = \{z; |z| = \varepsilon, \operatorname{Im} z \geqslant 0\}$ oriented clockwise and let $\mathscr{D}_{2,\varepsilon}$ be the contour shown in Fig. 6. Since

$$\int_{C_\varepsilon} dz \frac{\operatorname{ch} z}{\operatorname{sh}^3 z} \operatorname{cotg} \frac{z\omega}{\omega_p} = -\frac{2\omega_p}{3\omega\varepsilon^3} + \frac{2\omega}{3\omega_p \varepsilon} + O(\varepsilon) \tag{D7}$$

we see that (D5) reduces to

$$\begin{aligned} &\frac{\omega_p^2 - \omega^2}{6\omega_p \omega} + \frac{1}{2} \operatorname{Re}\left(\lim_{\varepsilon \to 0^+} \int_{\mathscr{D}_{2,\varepsilon}} dz \frac{\operatorname{ch} z}{\operatorname{sh}^3 z} \operatorname{cotg} \frac{z\omega}{\omega_p} \right) \\ &\quad = \frac{\omega_p^2 - \omega^2}{6\omega_p \omega} - \frac{\omega}{4\omega_p} \operatorname{Re}\left(\lim_{\varepsilon \to 0^+} \int_{\mathscr{D}_{2,\varepsilon}} dz \frac{1}{\operatorname{sh}^2 z \sin^2(z\omega/\omega_p)} \right) \end{aligned} \tag{D8}$$

After calculating the integral of $1/[\operatorname{sh}^2 z \sin^2(z\omega/\omega_p)]$ along $\mathscr{D}_{2,\varepsilon}$ by the theorem of residues, we find

$$\begin{aligned} &\mathscr{P}\mathscr{P} \int_0^\infty du \frac{\operatorname{ch} u}{\operatorname{sh}^3 u} \left[\operatorname{cotg}\left(\frac{u\omega}{\omega_p}\right) - \frac{\omega_p}{\omega} \coth u + \frac{\omega_p^2 + \omega^2}{3\omega_p \omega} u \right] \\ &\quad = \frac{\omega_p^2 - \omega^2}{6\omega_p \omega} - \frac{\pi\omega^2}{\omega_p^2} \sum_{n=1}^{\infty} \frac{\operatorname{ch}(n\pi\omega/\omega_p)}{\operatorname{sh}^3(n\pi\omega/\omega_p)} \end{aligned} \tag{D9}$$

Using (D9) and (D4) in (D2), we finally obtain the expression (4.45) for $r_{1,0}(\omega)$. Note that the series $\sum_{n=0}^{\infty} \cdots$ and $\sum_{n=1}^{\infty} \cdots$ converge exponentially rapidly. This allows simple and accurate numerical calculations of $r_{1,0}(\omega)$; for instance, $r_{1,0}(\omega_p)$ is determined with an absolute accuracy smaller than 10^{-4} by only keeping the first two terms of the previous series.

REFERENCES

1. A. Alastuey, *J. Stat. Phys.* **48**:839 (1987).
2. A. Lenard, *J. Math. Phys.* **2**:682 (1961).
3. H. Kunz, *Ann. Phys.* **85**:303 (1974).
4. Ph. Martin, Private communication; Ch. Lugrin and Ph. A. Martin, *J. Math. Phys.* **23**:2418 (1982).
5. Ph. A. Martin and Ch. Gruber, *J. Stat. Phys.* **31**:691 (1983).
6. J. P. Hansen and I. R. McDonald, in *Theory of Simple Liquids*, 2nd ed. (Academic Press, London, 1986).
7. J. Clerouin, J. P. Hansen, and B. Piller, to be published.
8. L. D. Landau, *J. Phys. (USSR)* **10**:25 (1946).
9. S. Ichimaru, *Basic Principles of Plasma Physics* (Benjamin, New York, 1973).